OPEN ACCESS
IOP Publishing | IMMT
International Journal of Extreme Manufacturing
Int. J. Extrem. Manuf. 1 (2019) 032002 (20pp)
https://doi.org/10.1088/2631-7990/ab3e54

Topical Review

Near-field acoustic levitation and applications to bearings: a critical review

Minghui Shi[1], Kai Feng[1,5], Junhui Hu[2], Jiang Zhu[3] and Hailong Cui[4]

[1] State Key Laboratory of Advanced Design and Manufacturing for Vehicle Body, Hunan University, Changsha 410082, People's Republic of China
[2] State Key Lab of Mechanics and Control of Mechanical Structures, Nanjing University of Aeronautics and Astronautics, Nanjing 210016, People's Republic of China
[3] Department of Mechanical Engineering, Tokyo Institute of Technology, Japan
[4] Institute of Machinery Manufacturing Technology, China Academy of Engineering Physics, Mianyang, 621000, People's Republic of China

E-mail: mh_shi@hnu.edu.cn, jkai.feng@gmail.com, ejhhu@nuaa.edu.cn, zhuj@mep.titech.ac.jp and cuihailong61@foxmail.com

Received 2 August 2019, revised 24 August 2019
Accepted for publication 25 August 2019
Published 12 September 2019

Abstract

The importance to industry of non-contact bearings is growing rapidly as the demand for high-speed and high-precision manufacturing equipment increases. As a recently developed non-contact technology, near-field acoustic levitation (NFAL) has drawn much attention for the advantages it offers, including no requirement for an external pressurized air supply, its compact structure, and its ability to adapt to its environment. In this paper, the working mechanism of NFAL is introduced in detail and compared to all existing non-contact technologies to demonstrate its versatility and potential for practical applications in industry. The fundamental theory of NFAL, including gas film lubrication theory and acoustic radiation pressure theory is presented. Then, the current state-of-the-art of the design and development of squeeze film air bearings based on NFAL is reviewed. Finally, future trends and obstacles to more widespread use are discussed.

Keywords: acoustic levitation, non-contact technology, bearing, measuring and manufacturing equipment, squeeze film

(Some figures may appear in colour only in the online journal)

1. Introduction

As the trend in equipment moves toward intelligent development, the requirement for highly accurate supporting elements for precise positioning systems, measuring instruments, and manufacturing equipment is increasing [1–4]. In particular, the accuracy and stiffness of the transportation and rotation system should keep up with the development of industrial technology. As core components, bearings directly affect the performance and service life of a system. Many non-contact technologies have been extensively developed to improve the rotation accuracy and stability of systems.

Currently available non-contact bearings include aerostatic and aerodynamic bearings, as well as magnetic bearings. However, these traditional bearings have many drawbacks. Aerostatic bearings require a clean air supply system during operation, which not only occupies more space but also increases the cost [5]. Aerodynamic bearings suffer severe friction and wear on the surface during the start-up and

[5] Author to whom any correspondence should be addressed.

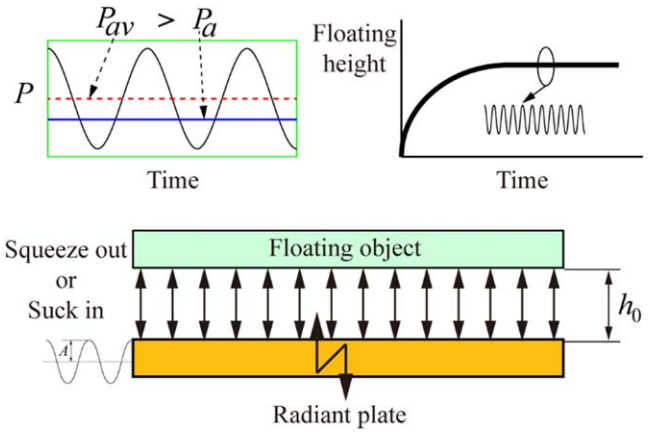

Figure 1. Schematic diagram of squeeze film levitation.

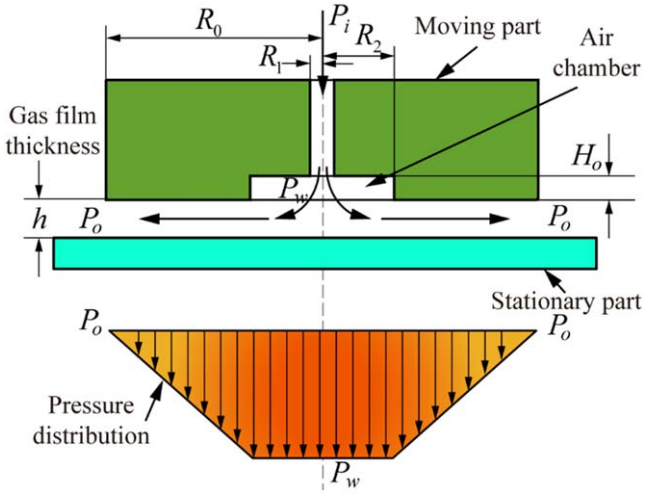

Figure 2. Schematic diagram of operating principle of aerostatic bearing.

stop stages [6–9]. Magnetic bearings not only need a complex structure to produce a strong magnetic field but also have an uncertain influence on the instrument/equipment due to the magnetic flux [10].

The squeeze film effect can be observed in many engineering instruments, e.g. in dampers, gudgeon pin bearings, gears, and lubricated parts of living bodies, etc. This working principle can be used to levitate objects, as shown in figure 1. If we put an object on a plane and drive the plane to vibrate in the direction normal to its surface with a vibration generator, the air within the gap between the plane and the object will be periodically sucked in and squeezed out. The time-averaged pressure for one period in the gap will be higher than ambient pressure and thus generating levitation force to support load and lift the object. This phenomenon is called near-field acoustic levitation (NFAL) (also called squeeze film levitation), which may overcome the drawbacks of traditional non-contact technologies.

In 1886, Reynolds [11] first explained that the squeeze effect was an important mechanism for the generation of pressure in lubricating film. However, since then, researchers have not appreciated the squeeze effect because there has been no suitable vibration generator. With the development of piezoelectric actuators, which can be used as high-efficiency vibration generators, the potential of squeeze film technology as a non-contact levitation method was rediscovered. In the 1960s, Tipei [12] investigated the gas squeeze film theory. Then, some theoretical and experimental works were reported by other authors [13–17], which validated the feasibility of squeeze film levitation. Since then, acoustic levitation has been investigated by researchers [18–20]. In recent years, many kinds of acoustic levitation equipments have been designed, manufactured, and widely applied in various fields, such as microassembly [21], biomaterials [22], analytical chemistry [23, 24], material sciences [25], and pharmaceuticals [26].

Some papers on squeeze film air bearings (SFABs) have been recently reported, which can provide us with a more comprehensive understanding of SFABs from both scientific and practical perspectives. The purpose of this review is not only to summarize theoretical modeling, the basic principle, structure design, and applications of NFAL, but, more importantly, to promote the application in engineering.

This review is organized into seven sections. In section 2, four types of non-contact bearing technologies are described and discussed, including aerostatic bearings, aerodynamic bearings, magnetic bearings, and SFABs. Section 3 reviews the history of the development of SFABs and summarizes the state of the art in NFAL theory. Section 4 summarizes several common types of SFABs. The operating principle of hybrid SFABs is introduced in section 5, pointing out that the working mode of this kind of hybrid bearing can be chosen freely according to the need. Discussion and future trends of SFABs are presented in section 6. Finally, conclusions are provided in section 7.

2. Working mechanism of several non-contact bearing technologies

Non-contact bearing technologies are widely used in high-precision measuring and manufacturing equipment due to the absence of contact and friction forces between stationary and moving components. Four types of non-contact bearing technologies are briefly described, focusing on their working characteristics and basic features.

2.1. Aerostatic bearings

Aerostatic bearings have been successfully used in high precision applications, e.g. precise moving devices, machine tools, manufacturing equipment, and measuring instruments, etc. Figure 2 shows a schematic diagram of a typical circular aerostatic bearing with a central orifice restrictor and a cylindrical recess. The radius of the bearing is R_0, R_1 is the radius of the supply orifice, and R_2 and H_0 refer to the size of the air chamber. The initial gas film thickness is h. Pressurized air is supplied through a central orifice-specific restrictor into the clearance between the stationary part and the surface of the bearing. The initial pressure of the inlet of the restrictor is P_i. After entering the chamber, the air pressure drops to P_w. Finally, the air is discharged to the surrounding ambient air

through the exit edges of the bearing gap; and the pressure gradually decreases to P_o. Aerostatic bearings are also called externally pressurized air bearings as the two surfaces are separated by an air film generated by an external air supply system.

The restrictor and pressure distribution in the clearance have an obvious influence on the load-carrying capacity and stiffness of aerostatic bearings. Therefore, studies on the restrictors and pressure distribution have been reported by many researchers. An aerostatic flat pad bearing with annular orifice restrictors was investigated by Stout [27] who showed that an aerostatic bearing with annular orifice restrictors was a better choice if the designer was concerned about pneumatic hammer instability. Stout *et al* [28] proposed a spherical gas bearing with slot restrictors. The optimum design conditions were determined by analyzing the bearing geometry and pressure ratio. The results showed that the bearing has a maximum radial load capacity when the design pressure ratio is in the region of 0.5. However, instability will occur when the direction of the eccentricity is toward any one slot.

Nakamura *et al* [29] presented experiments and predictions for an aerostatic rectangular thrust bearing with compound restrictors which combines a feed-hole restrictor with a groove compensation restrictor. In 1964, Mori *et al* [30] used a test rig to study the behavior of circular thrust gas bearings with a porous bearing surface. The pressure distribution and the load-carrying capacity were measured. Theoretical results showed good agreement with the experimental results. Since 1963, researchers such as Mori *et al* [31], Kassab *et al* [32], Yoshimoto *et al* [33] and Belforte *et al* [34] have studied the pressure distribution in the bearing clearance in order to improve the stiffness and load-carrying capacity of aerostatic bearings.

Aerostatic bearings can effectively overcome friction and wear issues during the working process. However, pneumatic hammer vibration [35] and vortex shedding [36] may occur during the working process. Furthermore, aerostatic bearings require a clean air supply system during operation, which not only occupying more space but also increasing the cost.

2.2. Aerodynamic bearings

Aerodynamic bearings work on the principle of aerodynamic effect, which is the best known pressure generation mechanism in the flow of a fluid. The operating principle of aerodynamic bearings is illustrated in figure 3. A tilting upper surface, W_1W_2, is stationary; and a lower surface, Z_1Z_2, is moving relative to the upper surface in the x direction with a velocity of u_1. The clearance is filled with gas lubricant. The entrance clearance and exit clearance between the two surfaces are h_0 and h_2, respectively. The gas film thickness at a certain point in the middle is h_1. When the lower surface moves at the velocity, u_1, the clearance along the direction of motion decreases gradually; and the fluid flows from the large clearance to the small clearance forming convergent clearance. The inflow fluid is more than the outflow fluid because h_0 is larger than h_2, and the flow is clearly discontinuous. Therefore, the pressure is generated by the viscous shearing of

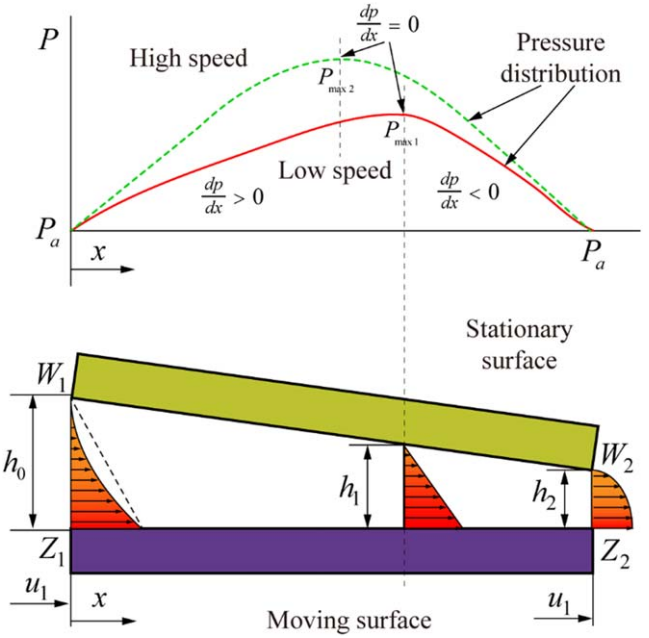

Figure 3. Schematic diagram of the operating principle of aerodynamic bearing.

gas film in the clearance, which is the source of load-carrying capacity. Note that if the stationary surface is parallel to the moving surface, there is no pressure generation between the two surfaces. In other words, the aerodynamic effect can only be generated when there is a tilting angle between the two surfaces. High relative speed can obviously enhance the aerodynamic effect.

Early research on air lubrication technology was conducted by Willis [37], who experimentally investigated the airflow status between two parallel plane surfaces. Then, the famous Reynolds equations, combining the simplified Navier-Stokes equations with a continuity equation, were proposed by Reynolds in 1886 [11]. In 1897, Kingsbury [38] verified the feasibility of a gas bearing through experimental research. The reference [39] combined the Reynolds equation and the compressible gas equations to present the basic calculation model for gas lubrication. After that, Katto and Soda [40] gave an analytical expression for the load-carrying capacity under the assumption of isothermal and infinitely long bearing conditions.

The load-carrying capacity and half-speed whirl are two important issues for aerodynamic bearings. The load-carrying capacity of an aerodynamic bearing is usually much less than that of oil-lubricated bearings due to the extremely low viscosity of air [41]. Half-speed whirl, which is caused by a self-excited film whirl, often occurs for high-speed aerodynamic bearings [42, 43]. This phenomenon is usually found to be the main reason for the instability of the rotor bearing system.

In order to improve bearing performance, researchers conducted their investigations into the air pressure distribution and supporting structures, respectively. A portion of researchers changed the air pressure distribution in the gap by introducing grooves into the bearing or rotor surface [44–48].

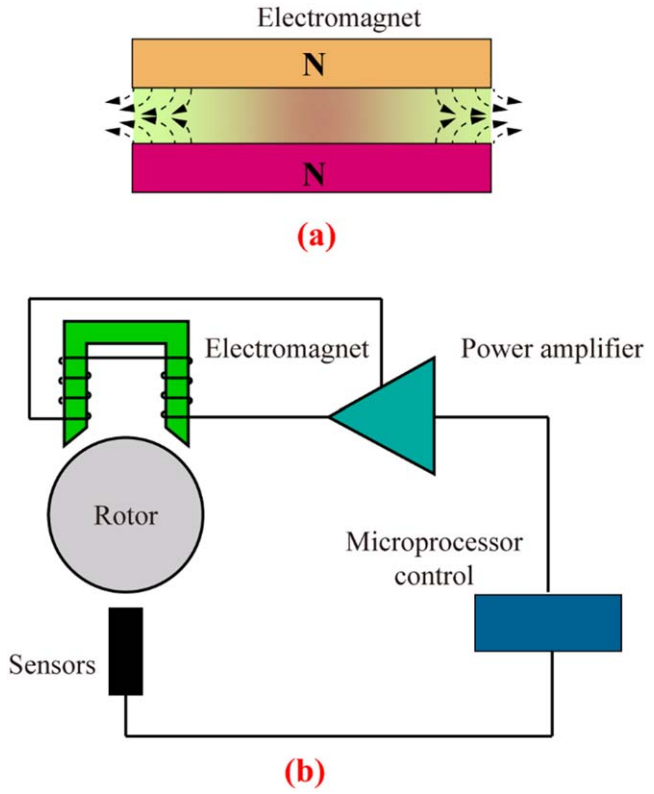

Figure 4. Schematic diagram of the operating principle of magnetic bearing, (a) schematic diagram of magnetic levitation and (b) active magnetic bearing.

Grooved bearings can enhance the load-carrying capacity and film damping effect. Other researchers changed the supporting structures by introducing a tilting pad or compliant metal material. Tilting pad gas bearings have been successfully used in high-speed rotating machinery due to their inherent stability [49–52]. Foil gas bearings, which have a flexible bearing surface constructed with a metal plate, are widely used in much turbomachinery [53–57]. However, wear between the top foil and shaft surface is inevitable for typical foil bearings; and thus routine maintenance needs to be conducted.

The gas film force of aerodynamic bearings is normally insufficient to support the rotor weight during the start-up and stop stages. Severe friction and wear will occur on the surface of aerodynamic bearings. The lifetime of aerodynamic bearings is directly dependent on the number of starts and stops.

2.3. Magnetic bearings

Magnetic levitation technology is a physical separation method which supports the object without any mechanical contact [58, 59]. A simple schematic of magnetic levitation is shown in figure 4(a). Magnetic bearings can be divided into three types according to their working principles: passive, active, and hybrid. Passive magnetic bearings do not need a control system but use their own permanent magnetic force or superconducting magnetic force to suspend the shaft, as shown in figure 4(a). Therefore, the stability region of passive bearing systems is very small since they have no damping characteristics [60–62]. Active magnetic bearings (AMBs)

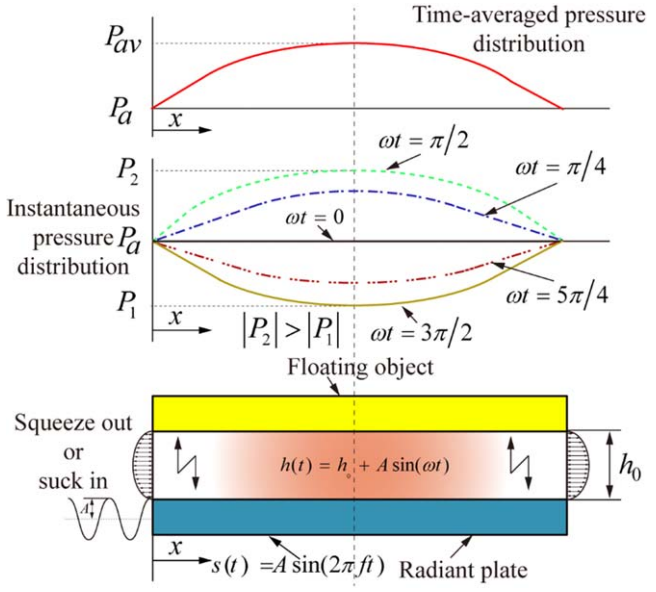

Figure 5. Schematic diagram of operating principle of squeeze film air bearing.

levitate the rotor by means of electromagnetic force. They are mainly composed of rotors, an electromagnet, sensors, controllers, and power amplifiers [63–66]. Figure 4(b) shows a schematic diagram of the working principle of an active electromagnetic bearing. The shaft deviation signal of the rotor is detected by the displacement sensor and sent to the controller. The current in the electromagnet is controlled by a power amplifier, so that the change in the electromagnetic force can make the rotor suspend in the specified position. Compared with passive magnetic bearing, the design of an AMB system is more complex; but its damping characteristics and stability are better. Hybrid magnetic bearing is a kind of combined magnetic bearing system that is formed on the basis of the AMB, passive magnetic bearing, and other auxiliary support and stable structures [67–69]. It uses the magnetic field generated by a permanent magnet to replace the static bias magnetic field of an electromagnet. Not only is the power consumption of the power amplifier significantly reduced, but the number of ampere turns of the electromagnet is reduced by half, the volume of the magnetic bearing is reduced, and the bearing capacity is improved.

2.4. Squeeze film air bearings

A schematic diagram of a system based on squeeze film levitation is shown in figure 5. The surface of the radiant plate, which is connected to the vibration generator, is driven to vibrate in the direction normal to the upper plate with high frequency periodic motion so that the air within the gap is periodically sucked in and squeezed out. To obtain optimal levitation performance of squeeze film levitation, the distance between the radiant plate and floating plate is required to be small enough to generate high gas pressure. Generally, the clearance of tens of microns is adopted, which is much smaller than the sound wavelength in air. The pressure in the gap varies periodically, and thus the pressure value is

Table 1. Advantages and disadvantages of non-contact bearings.

Non-contact bearings	Advantages	Disadvantages
Aerostatic bearings	Low friction loss, low heat generation, high motion accuracy, and long run time	Requires a large volume, continuous supply of clean air, and requires external auxiliary devices, and pneumatic hammer vibration
Aerodynamic bearings	Wide speed range, high rotational precision, and large temperature application range	High friction and wear during the start and stop stages of operation, relatively low stiffness and damping, and requires high machining accuracy and high assembly error
Magnetic bearings	Less frictional wear, low vibration, high rotational speed, usefulness in special environments, quietness, and low maintenance	Produces magnetic flux, cannot be used for magnetically sensitive configurations, and needs a stability control system
Squeeze film air bearings	Less frictional wear, levitation force at zero speed, high stability, and controllability	Bulk device, high energy consumption, and short run time

different at different times. The instantaneous pressure distribution and time-averaged pressure distribution between the two flat plates is shown in figure 5. The ambient pressure is set to P_a. The gas film pressure may be either negative or positive in one cycle, and the sign of the pressure value depends on the direction of the squeeze. In addition, the peak value of positive pressure is larger than the peak value of negative pressure ($|P_2| > |P_1|$). Therefore, time-averaged pressure in one period is greater than the ambient pressure, which is the reason for levitation force. Load-carrying capacity obtained from squeeze film levitation increases nonlinearly with the decrease in the film thickness.

The analysis of squeeze film levitation theory based on gas film lubrication theory started with the work of Tipei [12] who obtained the governing equation of squeeze film with three-dimensional velocity components on the bearing surface for a compressible and unsteady lubricating film. Since then, Langlois [13] deduced the equation governing the pressure for ideal gas under isothermal conditions and solved the time-dependent Reynolds equation by the perturbation method for a film in which fluid inertia is negligible. Beck and Strodtman [70] investigated the load-carrying capability of the finite journal bearing and solved the governing equation by two methods, i.e. a small-parameter analysis and a numerical finite-difference technique, which are approximate analytical solutions. Pan [16] and DiPrima [71] used asymptotic methods to study the characteristics of squeeze film bearings and also gave approximate solutions. However, the asymptotic methods have a very limited range for the analysis parameters, especially in extreme cases. Later, many researchers proposed different types of SFABs, which are presented in the following section.

2.5. Comparison of non-contact bearings

Each type of non-contact bearings has its own characteristics. A comparison (see table 1) among the four non-contact bearings was conducted to compare their abilities in run time, stability, friction and wear, motion accuracy, and energy consumption, etc. As can be seen, aerostatic bearings and aerodynamic bearings provide high motion/rotational accuracy and low heat generation because they use non-contact gas support. However, aerostatic bearings require a large volume, continuous supply of clean air and external auxiliary devices. Aerodynamic bearings have relatively low stiffness and damping, while aerodynamic bearings require relatively high machining accuracy and assembly error. Although magnetic bearings have the advantages of low vibration, quietness, and low maintenance, they cause magnetic flux and need the material properties of the shaft to meet their requirement. Moreover, they always need a stability control system. SFABs can effectively overcome friction and wear during the start-up and shut-down process and own high stability and controllability by operating the vibration component. Unfortunately, SFABs require a bulky device and have high energy consumption and a short run time because the high-frequency vibration of the vibration generator in the system generates heat.

3. Theoretical modeling

3.1. Governing equation based on gas film lubrication theory

Although a squeeze film levitation system is mainly composed of a radiant body and levitated object, the establishment of theoretical model is very complicated in reality. The reason lies in the levitated body's dynamic and the elastic deformation of the radiant surface, which is usually the modal shape of the structure. Looking into the history of squeeze film analysis, we found that the theoretical model has evolved from simple to complex (see figure 6). Due to the development of numerical calculation and analysis tools, the influence of the levitated body's dynamic and the elastic deformation of the radiant surface on the levitation performance is gradually considered in the model, leading to a deepening understanding of the working mechanism of squeeze film levitation.

The state of the levitated object is one of the important factors to be considered in the establishment of a theoretical model. The theoretical model (Model 1) in which the levitating object is fixed is used by many researchers

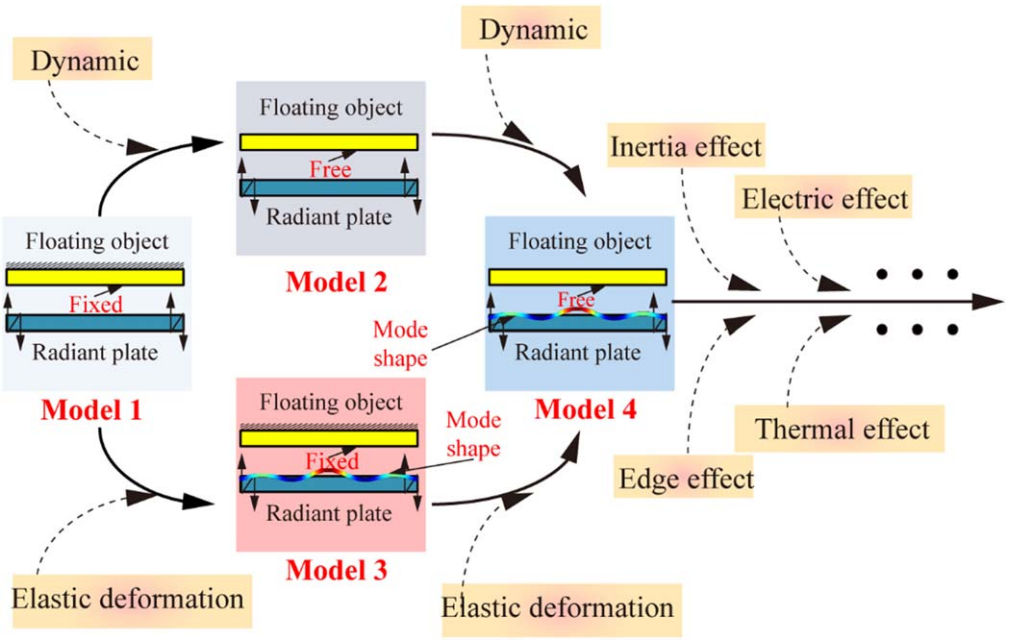

Figure 6. Gas film lubrication theory of squeeze film levitation.

[13, 15, 70–72]. However, the assumption that a levitating object is fixed is not reasonable because the movement of the levitating object is changed in the actual situation. In order to realize the squeeze levitation process more realistically, the dynamics of a levitating body are taken into account in the theoretical model (Model 2) [73–76].

Another issue with the theoretical model of squeeze films is the elastic deformation of the radiant surface. In the squeeze film levitation system, a better squeeze effect can be obtained at resonance frequency. Note that the magnitude of the gas film clearance is at the micron level. Therefore, the influence of the mode shape of the radiant body on the squeeze film effect cannot be ignored.

The conditions of more accurate models (Models 3 and 4) with the mode shape of the radiant body considered which have been presented by many researchers [77–81] are the subject of study because they comply with the real conditions of squeeze film levitation, particularly when working at a higher frequency. Based on their theoretical models, the theoretical results show good agreement with the experimental results.

A modified Reynolds equation considering the inertia effects of squeeze film was presented by several investigators [82–85]. Furthermore, Nomura and Kamakura [86] developed a model that includes viscosity and acoustic energy leakage. Later, a similar numerical study was conducted by Minikes *et al* [87] using a modified Reynolds equation. Minikes and Bucher [88] developed a theoretical model coupling the dynamics of a squeeze film levitated mass and vibrating piezoelectric disc. Moreover, Minikes and Bucher [89] introduced the release boundary condition and the isothermal assumptions into a squeeze film levitation model through a computational fluid dynamics scheme. It was found that the levitation force, when taking into consideration the energy leakage near the edges of the levitated object, was smaller by up to 50% compared to that of a one-dimensional analytical solution with the same boundary condition. Feng *et al* [90] introduced a grooving method into a squeeze film levitation system that was derived from bearing technology. They concluded that appropriate grooves can increase the levitation force.

Based on the usual assumption of lubrication theory, the Reynolds equation, which is a one-dimensional and time-dependent governing equation for pressure distribution in the squeeze film, can be obtained [91]:

$$\frac{\partial}{\partial X}\left(PH^3\frac{\partial P}{\partial X}\right)=\sigma\frac{\partial(PH)}{\partial T}, \tag{1}$$

where

$$P=\frac{p}{P_a},\ H=\frac{h}{h_0},\ X=\frac{x}{L},\ T=\omega\tau,\ \sigma=\frac{12\mu\omega}{P_a}\left(\frac{L}{h_0}\right)^2,$$

where P and H correspond to non-dimensional pressure and mean clearance normalized by ambient pressure (P_a) and gas film clearance (h_0), respectively. The dimensionless lateral coordinate is represented by Z; air viscosity and angular velocity of vibration are denoted by μ and ω, respectively; T is dimensionless time; τ is the time; L is the width of flat plane; and σ is the squeeze number.

Similarly, the two-dimensional Reynolds equation can be written as follows:

$$\frac{\partial}{\partial\theta}\left(PH^3\frac{\partial P}{\partial\theta}\right)+\frac{\partial}{\partial X}\left(PH^3\frac{\partial P}{\partial X}\right)=\sigma\frac{\partial(PH)}{\partial T}, \tag{2}$$

where the dimensionless axial coordinate and circumferential coordinate are denoted by X and θ, respectively.

Equations (1) and (2) contain only the squeeze film effect. The two-dimensional Reynolds equation containing

the squeeze film effect and the aerodynamic effect can be expressed as follows:

$$\frac{\partial}{\partial\theta}\left(PH^3\frac{\partial P}{\partial\theta}\right)+\frac{\partial}{\partial X}\left(PH^3\frac{\partial P}{\partial X}\right)=\Lambda\frac{\partial(PH)}{\partial\theta}+\sigma\frac{\partial(PH)}{\partial T}, \tag{3}$$

where Λ is the number of bearings and is represented by

$$\Lambda=\frac{6\mu\Omega}{P_a}\left(\frac{L}{h_0}\right)^2,$$

where Ω refers to the rotational speed of rotor.

The first right-hand term of equation (3) denotes the aerodynamic effect, which is generated by the physical wedge. The second right-hand term of equation (3) reflects the squeeze film effect that is generated by the cyclically squeezing action of the radiant body. The aerodynamic effect, squeeze film effect, and hybrid effects on the running characteristics of the squeeze film bearing are discussed in section 5.

3.2. Governing equation based on acoustic radiation pressure theory

The acoustic radiation pressure is the time-average pressure acting on a levitated object in a sound field, which was first computed by Loard Rayleigh [92]. Since then, many researchers have devoted themselves to the theory of acoustic radiation pressure [93–96]. Even if there are some improvements to the theoretical research, there is still some confusion and paradoxes in the theory of acoustic radiation pressure. The landmark work in which a formulation applied to calculate Rayleigh radiation pressure in ideal gas on a perfectly reflecting target was completed by Chu and Apfel [97]. Later, the theory of acoustic radiation pressure was extended and generalized by Lee and Wang [98]. The expression derived by Chu and Apfel for Rayleigh radiation pressure is given as follows:

$$p=\langle P-P_0\rangle=\frac{1+\gamma}{2}\left(1+\frac{\sin(2kh)}{2kh}\right)\langle E\rangle \tag{4}$$

$$\langle E\rangle=\left(\frac{a_0^2}{4}\right)\left(\frac{\rho_0\omega_0^2}{\sin^2(kh)}\right),\quad k=\frac{\omega}{c}, \tag{5}$$

where $\langle\rangle$ stands for time averaged values, γ, h, k, a_0, ρ_0, ω_0, and c are the specific heat ratio of the medium, distance between two surfaces, wave number, vibration amplitude, density of the medium, angular velocity of the wave, and speed of sound, respectively. The energy density is represented by E.

When the levitation distance is in the micrometer range, it is much smaller than the sound wavelength in the free field. Therefore, equation (4) can be simplified to a linear equation for radiation pressure in the following form:

$$\Upsilon=\frac{1+\gamma}{4}\rho_0c^2\frac{a_0^2}{h^2}, \tag{6}$$

where $\sin(kh)\approx kh$ is assumed. From equation (6), it can be concluded that the vibration amplitude and levitation distance are two crucial parameters for a squeeze film levitation system. Equation (6) is usually used in the study of a squeeze film levitation system for transportation or rotation. Its validity has been verified by the investigators through experiments [99, 100]. Experimental values agree well with theoretical values based on equation (6).

Furthermore, for a squeeze film levitation generated by flexural vibration, the particle velocity amplitude distribution is written as

$$v(x,y,z)=\frac{1}{4\pi^2}\iint\hat{v}(k_x,k_y)\times\exp\left[\mathrm{j}(k_xx+k_yy+k_zz)\right]dk_xdk_y. \tag{7}$$

Here, $k_x^2+k_y^2+k_z^2=k_a^2=(\omega_0^2/c_a^2)$, k_x, k_y, and k_z are the wave vector components along the x, y, and z directions, respectively. The radiation pressure of a plane wave in the z direction can be obtained:

$$p(k_x,k_y)=\frac{1+\gamma}{2}\left(1+\frac{\sin(2k_zh)}{2k_zh}\right)\langle E_z(k_x,k_y)\rangle \tag{8}$$

$$\langle E_z(k_x,k_y)\rangle=\frac{\rho_a\hat{v}^2(k_x,k_y)}{4\sin^2(kh)}. \tag{9}$$

Thus, the total radiation pressure can be expressed as follows [100]:

$$\Upsilon|_{z=h}=\iint_{k_x^2+k_y^2<k_a^2}p(k_x,k_y)dk_xdk_y. \tag{10}$$

3.3. Comparison of two theories

The two methods mentioned above have their own characteristics. The squeeze film levitation model based on gas film lubrication theory can be used to describe purely viscous air in a gap. However, this method is limited to cases with extremely small levitation distances. The squeeze film levitation model established by acoustic radiation pressure theory is limited to cases where the gas viscosity is negligible. Zhao *et al* [101] made a comparative analysis of the two methods to see their prediction accuracy. They found that the squeeze film levitation model based on gas film lubrication theory obtained a satisfactory fit for small gap distances, but the model based on acoustic radiation pressure theory got a satisfactory fit for a relatively large distance. When the levitation distance increases to a certain extent, the two methods fail to agree with the measured values. In 2016, Melikhov *et al* [102] developed a theoretical model, including the viscous and acoustic effects, which can be applied for a wide range of levitation heights.

4. Different types of SFABs

Because of the advantages mentioned above, SFABs with different functions have been proposed by investigators, such as squeeze film air linear bearings, squeeze film thrust bearings, and squeeze film spherical bearings.

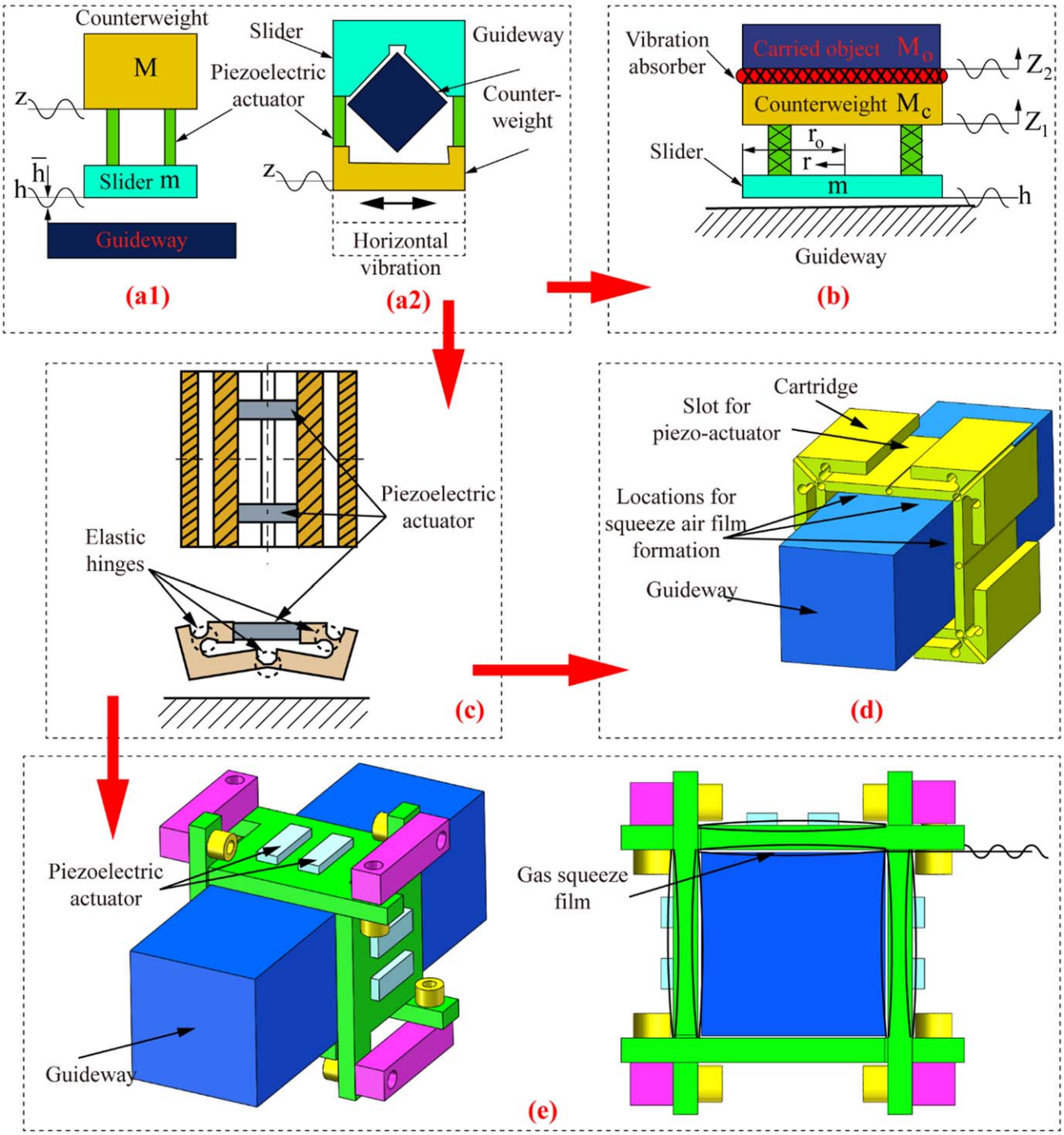

Figure 7. Schematic diagram of squeeze film air linear bearing: (a) Yoshimoto and Anno [103], (b) Yoshimoto [104], (c) Yoshimoto *et al* [74], (d) Stolarski and Chai [105], and (e) Yoshimoto *et al* [78]. (a) Reproduced with permission from [103]. (b) Reproduced with permission from [104]. Copyright © 1997 by the American Society of Mechanical Engineers. (c) Reproduced with permission from [74]. © The Japan Society of Mechanical Engineers. (d) Reprinted from [105], Copyright (2006), with permission from Elsevier. (e) Reprinted from [78], Copyright (2007), with permission from Elsevier.

4.1. Squeeze film air linear bearings

Yoshimoto and Anno [103] proposed a rectangular squeeze film air gas bearing with a counterweight, as shown in figure 7(a1). The proposed bearing consists of a slider and counterweight, which are connected together by piezoelectric elements. Squeeze film pressure was generated between the surface of the slider and guideway. Furthermore, the authors designed a new bearing guideway system based on the proposed bearing for a linear motion guide (see figure 7(a2)). Experiments were performed to successfully investigate the floating characteristics of the bearing. Stable levitation of a counterweight of about 0.4 kg levitated by the bearing with 450 mm^2 was achieved. However, the levitated object oscillated together with the counterweight, which was detrimental to the motion accuracy of the levitated object.

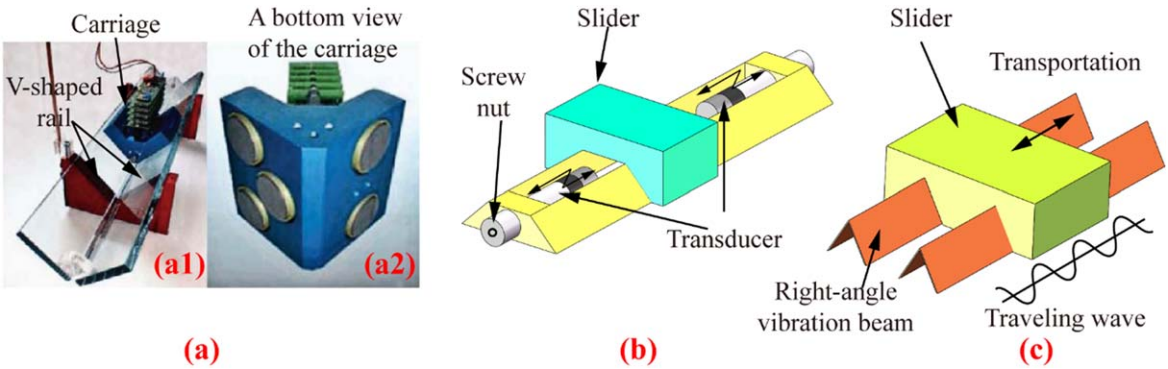

Figure 8. Schematic diagram of linear slider bearing: (a) Wiesendanger [106], (b) Ide *et al* [107], and (c) Ide *et al* [108]. (a) Reproduced with permission from [106]. (b) Reproduced from [107]. Copyright © 2005 The Japan Society of Applied Physics. All rights reserved. (c) Reprinted from [108], Copyright (2007), with permission from Elsevier.

To solve this problem, a new squeeze film gas bearing with a vibration absorber, which can be used to reduce the vibration amplitude of the levitated object and improve the motion accuracy, was proposed in [104]. As shown in figure 7(b), a vibration absorber made of silicone rubber was inserted between the counterweight and the carried object. Numerical and experimental results showed that the absorber was effective in reducing the vibration amplitude of the carried object.

Later, a new type of squeeze film gas bearing with elastic hinges for linear motion guide systems was proposed by Yoshimoto *et al* [74], as shown in figure 7(c). The bearing consists of three elastic hinges and two piezoelectric actuators, which produces a greater amplitude than the previous bearing proposed in [103] due to the use of elastic hinges. Meanwhile, this bearing increased its miniaturization because a counterweight and a horizontal fixing mode of the piezoelectric actuators were used.

Following the research of Yoshimoto on bearings with elastic hinges, Stolarski and Chai [105] proposed a novel linear motion sliding bearing using elastic hinges. The profile of the linear motion sliding is shown in figure 7(d). The proposed bearing consists of a specially shaped cartridge which can be conveniently divided into eight identical parts. Four actuators are mounted on each slot for generating a squeeze film effect at four converging gaps between the cartridge and the guideway. The structure of the proposed bearing is similar to the design in figure 7(c). However, the difference is that there are four slots for installing piezoelectric actuators rather than two. For the bearing proposed in figure 7(c), noise will be generated during operation due to the low frequency of operation. In order to solve this problem, a new square SFAB operated in the ultrasonic regime to avoid the generation of noise was presented in [78] (see figure 7(e)). The proposed bearing consists of four plates which are mounted by a screw. Note that only piezoelectric actuators are mounted on the top and two sides. Thus, the upper gas film pressure is the main power to produce the load-carrying capacity. However, the gas film pressure on the two sides only maintains the horizontal position of the slider. Experimental results show that the load-carrying capacity of 10 N is achieved, in the case of an average film thickness of 5 μm.

A linear slider bearing using disc-shaped piezoelectric bending elements was proposed [106]. The linear slider bearing consists of a V-shaped rail made of two glass plates and a carriage (see figures 8(a1) and (a2)). The opening angle of the rail is set to 90 degrees, and the five bearing modules are mounted on the carriage. A total load-carrying capacity of 30 N was obtained when driven at 24 volts.

After that, Ide *et al* [107] proposed a new low-profile design using two flat beams excited by two Langevin transducers for a linear bearing, as shown in figure 8(b). Two flat long beams connected to two '+' -shaped vibration converters with screws were used as a guide rail. The angle of the two output surfaces of the vibration converter was set to 45 degrees. A Langevin transducer excited by a two-phase sinusoidal voltage source was used to drive the beams. A slider was levitated by the squeeze gas film generated by bending vibrations excited along the beams. For this bearing, a further study was conducted by Koyama *et al* [109]. The levitation force (4.8 kN m^{-2}) and the levitation rigidity (2.5 kN μm^{-1} m^{-2}) were measured for a levitation distance of 2.2 μm. The maximum thrust and the transportation speed were also measured to be 1.3 mN and 34.6 mm s^{-1}, respectively, for a case of the slider's weight of 107 g. In [108], a linear bearing consisting of a pair of right-angle beams and Langevin transducers was designed (reference figure 8(c)). The Langevin transducers were mounted on the end of the beam by a screw, which can be used to excite and absorb ultrasonic flexural vibrations, forming a flexural traveling wave along the $\wedge$-cross-sectioned beam. A transportation speed of 138 mm s^{-1} of a 90 g slider supported by right-angle beams was obtained.

The design and testing of a linear rectangular air bearing using squeeze film generated by ultrasonic oscillation was performed in as described in [110]. The main structure of the proposed bearing was a horn consisting of two directional converters, shown in figure 9(a), which transmitted the oscillations of the two actuators to eight bearing surfaces. The squeeze film generated between the surface of the bearings and the surface of the carriage (see figure 9(b)) can be used to lift and guide the carriage. Experiments were conducted on a test rig to investigate the performance of the bearing. The 0.18 μm p–p of the vertical straightness error was obtained in the experiments.

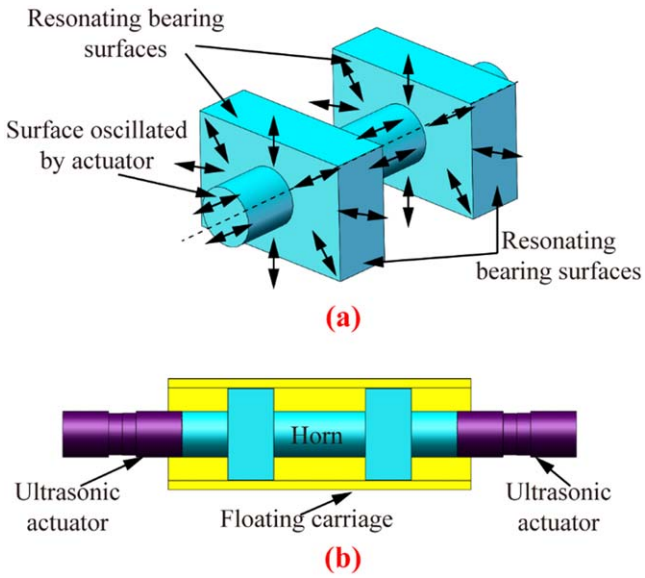

Figure 9. Schematic diagram of linear rectangular air bearing: Oiwa and Suzuki [110]. Reprinted from [110], with the permission of AIP Publishing.

4.2. Squeeze film thrust bearings

A squeeze thrust bearing was produced between two parallel, coaxial, flat disks, one of which was a rotor with flat disks and the other was driven sinusoidally in a direction normal to the surface [15]. A flat disk squeeze film bearing that utilizes air films generated by ultrasonic oscillation was reported in [73]. Similarly, the proposed bearing contains two parallel and coaxial flat disks. The upper disk is levitated by the levitation force generated by a high frequency squeezing motion of the lower plate driven by a piezoelectric ceramic cylinder.

In [111], an ultrasonic thrust bearing composed of a surface pulley and radiation surface of the piezoelectric transducer was proposed. The surface of the piezoelectric transducer can be used directly as the bearing surface. Squeeze gas film generated by the ultrasonic vibration of the piezoelectric transducer was used to support the weight of the shaft and the axial load (see figure 10(a1)). An ultrasonic thrust bearing and experimental device were manufactured. Experimental results showed that ultrasonic thrust bearing has better levitation and antifriction performance than a sliding bearing and non-liquid friction rolling bearing.

Song *et al* [112] developed a novel ultrasonic thrust bearing which was an improvement over the previous bearing described in [111]. The radiation surface of the piezoelectric transducer was designed as a conical structure and different from the surface of the cylindrical structure with the circular planar in the previous bearing (see figures 10(a2) and (b)). Moreover, the radiation pressure generated by the surface of the conical structure can carry radial and axial loads simultaneously. Experimental results indicated that the proposed ultrasonic thrust bearing was more suitable for high speed work environments.

4.3. Squeeze film spherical bearings

A novel spherical squeeze bearing based on NFAL is presented in [15]. The piezoelectric cylinder oscillates in a high frequency, which causes the socket to oscillate. Thus, a squeeze film is produced in the gap that makes the ball float freely. In [72], a spherical squeeze film bearing was designed. The proposed bearing consists of a hemisphere and a bearing shell, which are made of duralumin. When the bearing is working, the second mode of the bearing shell is excited. In [113], a transducer with a concave spherical surface which can be used to levitate a ball was designed (see figure 11). The appropriate concave spherical radiating surface of the proposed transducer was determined by the finite element parametric method. The levitation height and levitation perturbation of the ball were investigated. The experiments revealed that the maximum levitation height and minimum levitation perturbation were obtained when the radius of the levitated ball was similar to that of the concave spherical radiating surface.

A transducer which can be used to suspend high-mass rotors was designed in [114] (see figure 12). The horn on the top of the transducer has a concave surface which can be used to suspend spherical rotors with a diameter of about 40 mm. Experimental results indicated that a sphere weighing 1 kg was successfully suspended. For the NFAL, the attenuation motion of spherical rotors was further investigated in [115]. The experiment's results revealed that the maximum rotating speed and duration time of the spherical rotor were 6000 rpm and 15 min, respectively.

In [116], the authors describe a novel spherical bearing using a bowl-shaped non-contact ultrasonic motor with a hollow bowl-shaped surface that can be used to produce acoustic levitation force for a spherical object (see figure 13). A piezoceramic ring divided into two groups was used to excite the stator. When two high-frequency AC voltages with a temporal phase shift of 90° were applied to the piezoceramic ring, a traveling wave was produced in the spherical surface of the stator, resulting in a load-carrying squeeze film which can levitate or even directly drive a spherical rotor to rotate without contact. A maximum rotating speed of about 1071 rpm was obtained for the proposed spherical bearing. Experimental results indicated that the proposed bearing has potential application for suspended gyro.

5. Hybrid SFABs

5.1. Characteristics of hybrid SFABs

In high-speed applications, the aerodynamic effect as well as the squeeze film effect are included in the operation process. Thus, SFABs can be classified into two types, namely, SFABs (only squeeze film effect) and hybrid SFABs (combined squeeze film effect and aerodynamic effect). The schematic diagram in figure 14 represents the parameter status of hybrid SFABs and their operating principles. The three

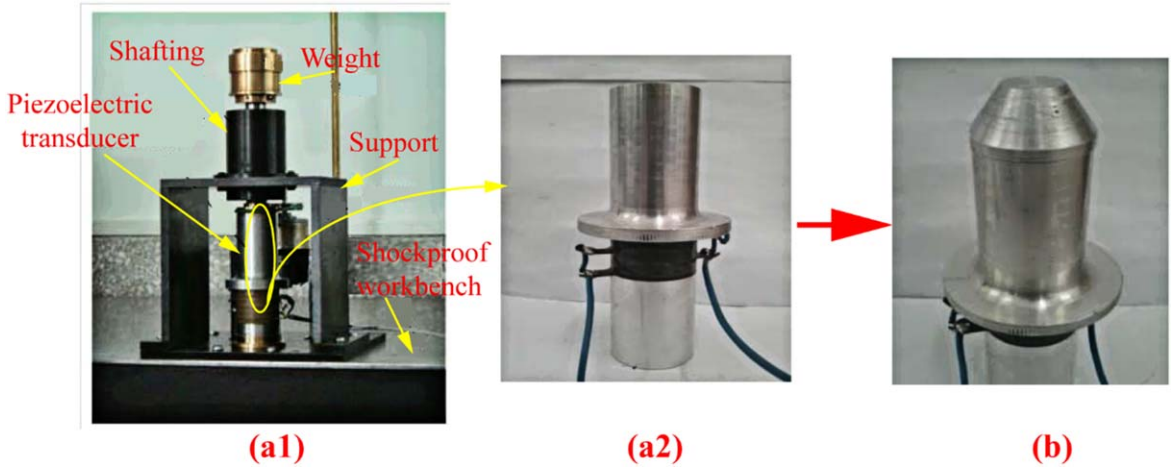

Figure 10. Photograph of ultrasonic suspension thrust bearing and piezoelectric transducers: (a) Shiju *et al* [111], and (b) Song *et al* [112]. (a) © 2015 IEEE. Reprinted, with permission, from [111]. (b) Reproduced with permission from [112].

Figure 11. Photograph of the transducer with concave spherical surface: Liu *et al* [113]. [113] © The Korean Society of Mechanical Engineers and Springer-Verlag Berlin Heidelberg 2013. With permission of Springer.

vertical dotted lines divide the schematic diagram into three working areas.

The levitation force generated by the squeeze film effect in Region I can effectively support the rotor. When the levitation force on the rotor is larger than the gravity of the rotor, the bearing can overcome the wear during start-up. Thus, compared with a conventional non-contact aerodynamic bearing, the service life of a hybrid SFAB can be greatly improved.

In Region II, when the rotor begins to rotate, the aerodynamic effect gets to work due to the relative speed between the rotor and bearing surface. The levitation force produced by squeeze film effect and aerodynamic effect supports the rotor, simultaneously. The aerodynamic effect increases with the increase in rotating speed, which leads to an increase in load-carrying capacity. Afterwards, the rotor speed gradually reaches a constant value in Region III. In this region, the speed remains constant; and the input voltage can be selected according to the working conditions. The load-carrying capacity produced by hybrid SFABs results in a higher value than that produced by conventional aerodynamic bearings at the same speed due to the squeeze film effect enhancing the load-carrying capacity. Throughout the three steps, the rotor is levitated stably and the running performance of the bearing can be controlled by adjusting the input signal to vibration generator. In addition, it must be emphasized that the working mode of SFABs should be combined according to the actual working needs.

The main features of hybrid SFABs are listed and described as follows:

- No dry friction and wear during the start-up and shutdown stages.

  When the levitation force produced by the squeeze film effect is large enough, the rotor can be effectively supported. Therefore, compared with the traditional aerodynamic bearing, the SFAB can effectively avoid the friction and wear caused by the start-up and stop stages.
- Enhanced load-carrying capacity.

  Load-carrying capacity of hybrid SFABs is enhanced by introducing the squeeze film effect into the aerodynamic effect, especially in large eccentricity.
- Good stability with the help of the squeeze film effect.

  A traditional aerodynamic bearing will lose stability at a specific speed due to its cross-coupled stiffness. However, the force generated by the squeeze film effect will suppress the rotor vibration and improve the stability.
- Active controllability.

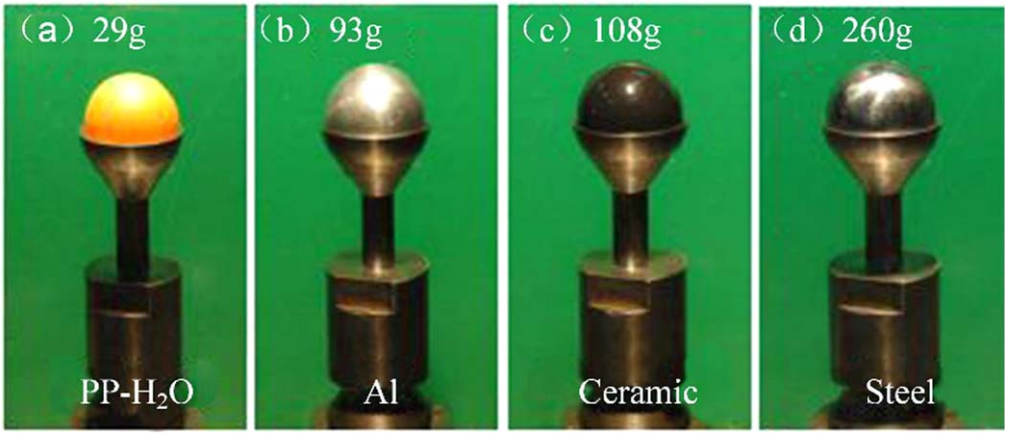

Figure 12. Photographs of different spherical rotors being levitated: Hong *et al* [114]. Reprinted from [114], with the permission of AIP Publishing.

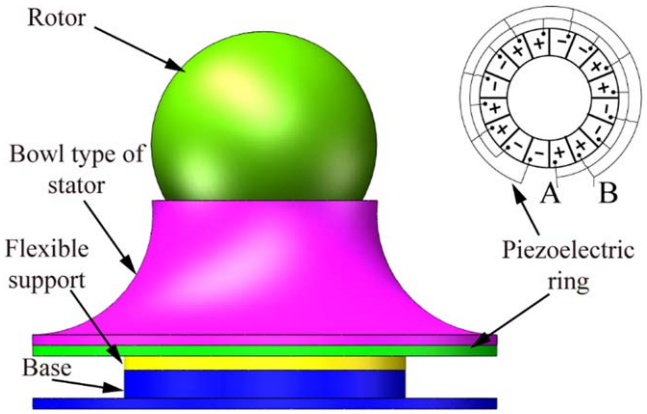

Figure 13. Schematic diagram of non-contact spherical bearing: Chen *et al* [116]. Reproduced with permission from [116].

The stable position of the rotor can be controlled by adjusting the vibration of the actuator and the levitation force from the squeeze film effect.

5.2. Different types of hybrid SFABs

Salbu [15] proposed a hybrid squeeze film air journal bearing with the journal squeeze film effect and squeeze thrust effect. Levitation forces were generated by high frequency movement of the piezoelectric cylinders and the flat piezoelectric disk. Later, a cylindrical squeeze-film journal bearing with a radially poled piezoelectric sleeve which provided radial squeeze film motion was proposed [17]. In this bearing, a double layer squeeze film was formed on the inner and outer surfaces of the sleeve-type transducer. Farron *et al* [117] proposed a novel SFAB which mainly consisted of a rotating member, strain producing tube, and support frame (see figure 15). The heart of the bearing was a strain producing tube, which could produce high frequency and low amplitude motion in directions both parallel and perpendicular to the axis of the rotating member. A double layer of squeeze film could be produced by squeeze motion perpendicular to the axis, which was squeeze film in Gap A and squeeze film in Gap B. Squeeze film A allowed the rotating member to rotate without friction, while squeeze film B played a supporting role in the strain-producing tube. In addition, the squeeze motion parallel to the axis produced squeeze film at both ends of the strain-producing tube. Therefore, the squeeze film bearing could provide both a radial support force and axial support force. In [118], a piezoelectric oscillating bearing supported by a pair of contiguous discs was developed. Two disks produced the opposite strain along the axis. In other words, one produced expansion and the other produced contraction. Therefore, a relatively large amplitude of motion was imparted to the bearing as there was no relative motion between the facing surfaces of the two discs.

Hu *et al* [119] designed and fabricated an ultrasonic bearing prototype which was actuated by two Langevin transducers driven by two AC voltages with a phase difference of 90°, as shown in figure 16. The two Langevin transducers were bolted on the stator with a distance of three quarters of wavelength. A traveling wave, which was used to drive the rotor rotation, was generated in the surface of the stator. Therefore, the radial support and rotation of the rotor could be realized by the force generated by the traveling sound field.

An active squeeze air bearing based on ultrasonic oscillation was proposed in [120], as shown in figure 17. A directional converter was used by the bearing to transmit the oscillation of Langevin transducer to both an end surface and a side surface. In other words, the converter could generate radial and axial squeeze motion, respectively. A test rig, which consisted of a bolt-clamped Langevin transducer, a rotor, and a directional converter, was built to investigate the motion error compensation characteristic of the bearing. The movement of a master ball supported by the rotor was measured by a fiber optic displacement sensor. This PI feedback control with compensation provided lower axial runout than PI feedback control without compensation.

An aerodynamic bearing with adjustable geometry, as shown in figure 18(a), was studied [77]. The shape of the inner surface of the bearing could be changed from initial cylindrical to three-lobed due to the use of elastic hinges. Six piezoelectric actuators were installed in three slots evenly

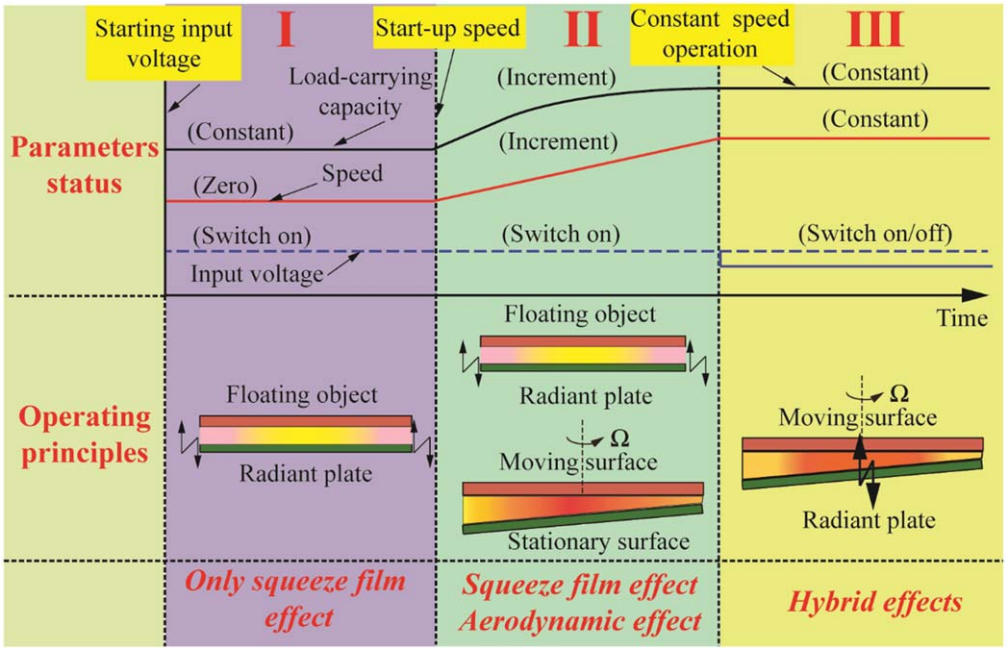

Figure 14. Schematic diagram of operating steps of hybrid squeeze film air bearings.

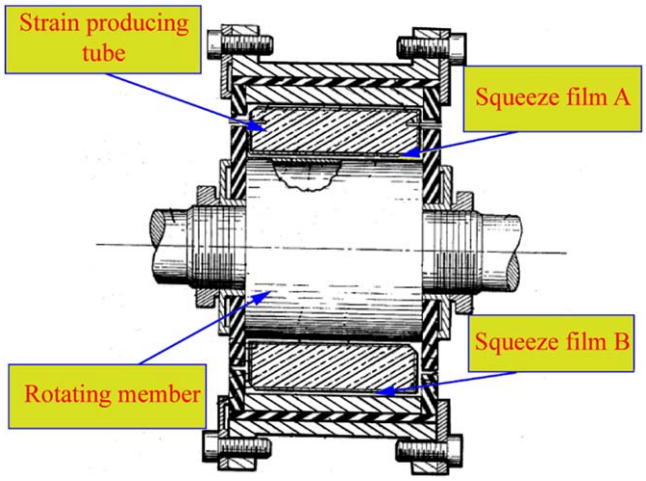

Figure 15. Bearing structure assembly schematic: Farron *et al* [117]. Reproduced with permission from [117].

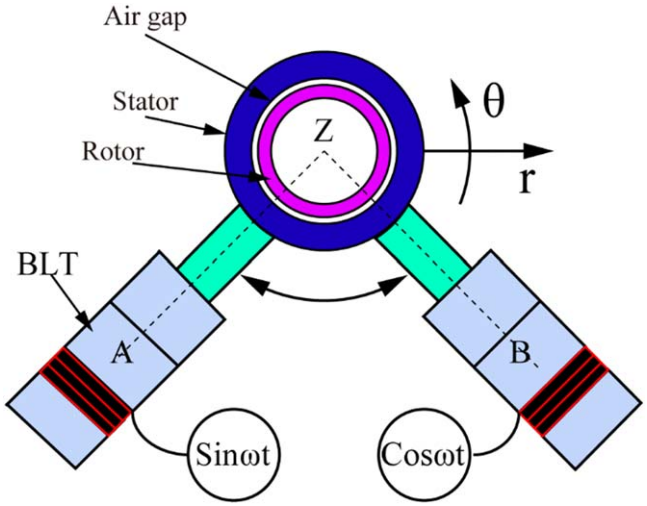

Figure 16. Schematic diagram of ultrasonic bearing: Hu *et al* [119]. Reprinted from [119], Copyright (1997), with permission from Elsevier.

distributed around the circle. Piezoelectric actuators periodically squeezed the gap between the bearing and the rotor, forming a layer of gas film pressure, and the rotor was suspended. In 2011, Stolarski [122] experimentally and numerically investigated the dynamic characteristics of the bearing. Comparing the theoretical and experimental results, it was found that the squeeze film effect generated by squeeze motion could significantly extend the threshold speed of instability. Later, the systematic analysis of the levitation mechanism and stability of the bearing at a higher operating frequency was carried out by Feng *et al* [123]. In [121], the authors presented a similar bearing with [77] (see figure 18(b)). The influence of the squeeze film effect on the running performance of the rotor to this bearing was studied by Stolarski *et al* [124]. Experimental results showed that the squeeze film effect had an obvious effect on reducing rotor vibration. It was noticed that at a constant running speed (20 000 rpm) and external load (0.31 N), the shaft vibrations were reduced by approximately 37.5% and 42% in the x and y directions, respectively.

In [125], three different types of air journal bearings utilizing NFAL were designed from the perspective of a simplified structure and elastic bore deformation (see figure 19). The resonance frequency and vibration mode were determined using ANSYS. The squeeze film load capacity of these bearings was tested through a specially built test rig. Theoretical and experimental results showed that a journal bearing using acoustic levitation is feasible and has potential applications, especially for light loads, cleanliness, and compactness requirements. Furthermore, they concluded that

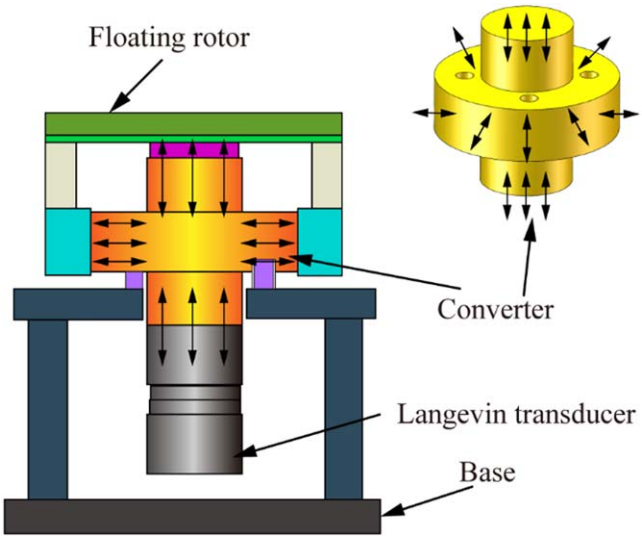

Figure 17. Schematic diagram of active squeeze film bearing: Oiwa and Kato [120]. Reprinted from [120], with the permission of AIP Publishing.

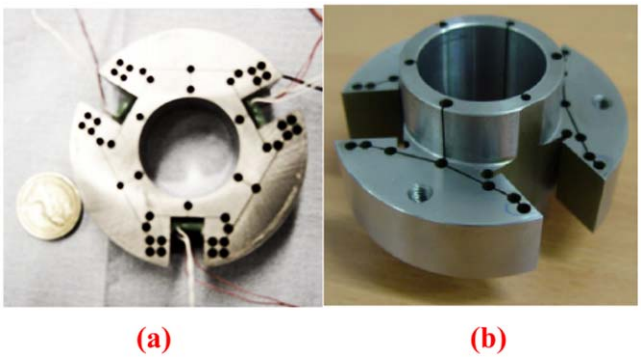

Figure 18. Photographs of acoustic bearing: Stolarski *et al* [77, 121]. (a) Reproduced with permission from [77]. (b) Reprinted from [121], Copyright (2015), with permission from Elsevier.

the bearing of Design 3 showed better characteristics. Therefore, the running performance of the bearing of Design 3 was studied by Shou *et al* [126]. The experimental results showed that for a given external load, the threshold speed of the bearing running without the squeeze film effect was 5000 rpm while the threshold speed for the bearing operating with the squeeze film effect was 20 000 rpm. Clearly, the squeeze film effect can significantly contribute to the dynamic stability of an aerodynamic bearing, especially for lightly loaded, gas-lubricated bearings. Later, a SFAB similar to Design 1 in [125] was proposed [127]. The proposed journal bearing equipped with three 20 mm long longitudinal fins requires the use of six piezoelectric actuators arranged around the circumference of the outer surface of the bearing.

In 2013, a SFAB with high load-carrying capacity with the ability of precision spindle position control was presented in [101] (see figure 20). The bearing consisted mainly of three Langevin-type transducers which were specially designed and fabricated. Three transducers, each covered 100° of a cylindrical surface, were positioned 120° apart on a housing. The spindle was supported by the arced concave radiation surface of the three transducers which were driven in the first longitudinal mode. It was noticed that each radiation surface was an independent vibration surface. The position trajectory of the spindle could be controlled by modulating the vibration amplitude of the corresponding transducer. The maximum load-carrying capacity of 51 N was obtained, and a position accuracy of the spindle center was achieved in the range of 100 nm. The simulation and experimental results showed that the proposed squeeze film journal bearing could be used for ultra-precision machining processes.

Wang *et al* [128] proposed an ultrasonic bearing with levitation and position functions. The bearing consisted of a bearing housing, a vibrating cylindrical stator, and two circular plates, as shown in figure 21. Acoustic levitation force which provided radial non-contact support for the rotor was produced by piezoelectric actuators squeezed on the cylindrical stator surface. The support in the axial position was provided by the force formed by the squeezing vibration of the circular plates. The proposed ultrasonic bearing that was able to levitate a rotor weighed 1.2 N and had potential application values for the support of the high precision gyros.

An ultrasonic levitating bearing excited by three piezoelectric transducers was developed as described in [129], and shown in figure 22. One distinct property that distinguished the proposed bearing from a previous bearing, described in [101], was that the bearing had the ability to self-align and carry radial and axial loads simultaneously due to the proper design of transducer structure. A maximum radial load of 15 N and an axial levitating load of 6 N were obtained from the established test system. Theoretical and experimental results showed that the proposed bearing provided a better method for bidirectional supporting capacity. Later, the friction characteristics and running stability of the bearing were studied, as described in [130, 131]. The friction torque increased with an increase in rotational speed, and torque of less than 120 μNm was obtained at 20 000 rpm. In addition, experimental results showed that the ultrasonic bearing could run stably in the speed-down and speed-up processes.

Feng *et al* [132] presented a novel SFAB with flexure pivot-tilting pads, as shown in figure 23. The pads were connected to the bearing housing through a straight beam and flexural web. The radical force was generated by squeezing the gas between the pads and rotor periodically using piezoelectric actuators. This bearing had two distinct advantages, which were different from previous squeeze film bearings. First, the bearing always adapted well to squeeze actions. Second, the proposed bearing had a better stability when the bearing worked at high speed due to low cross-coupled stiffness. Numerical and theoretical results showed that it was feasible for the proposed bearing to support high-speed and high-precision shafts. Shi *et al* [133] theoretically and experimentally identified the influences of material characteristics on the levitation performance of squeeze film bearing. The selection of squeeze film bearing material characteristics is important for the levitation performance. The test bearings that were comprised of two different materials (AL 2024 and 60Si2Mn) had similar resonance frequency and different vibration amplitudes generated by the

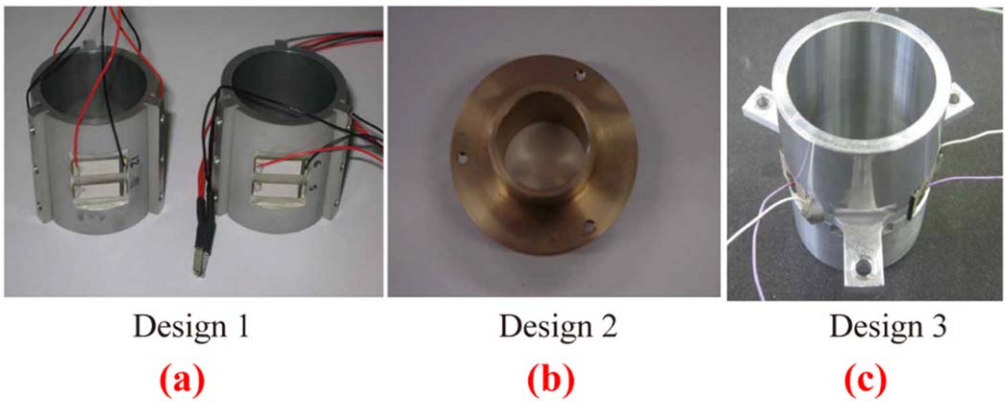

Figure 19. Photographs of air journal bearing using NFAL: Stolarski *et al* [125]. Reproduced with permission from [125].

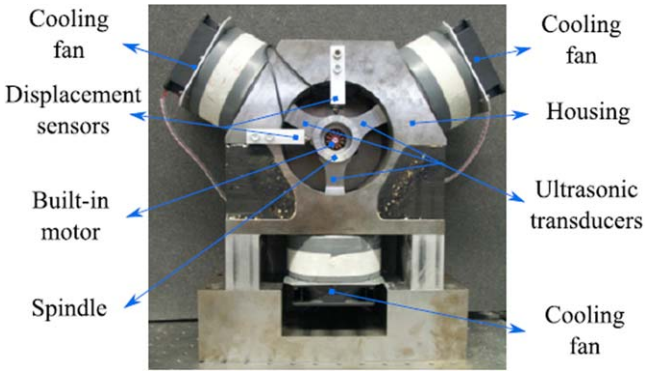

Figure 20. Photograph of ultrasonic levitation journal bearing: Zhao *et al* [101]. Reprinted from [101], Copyright (2013), with permission from Elsevier.

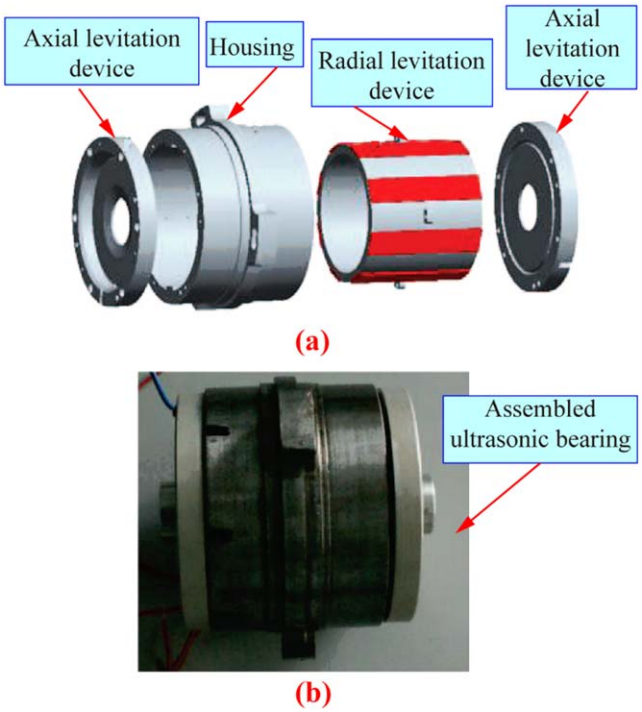

Figure 21. Exploded view and assembling drawing of ultrasonic levitation bearing: Wang *et al* [128]. © 2013 IEEE. Reprinted, with permission, from [128].

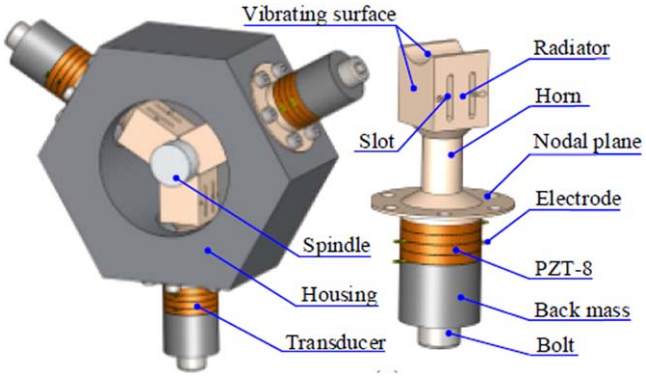

Figure 22. Schematic diagram of ultrasonic levitation bearing: Li *et al* [129]. Reproduced from [129]. CC BY 4.0.

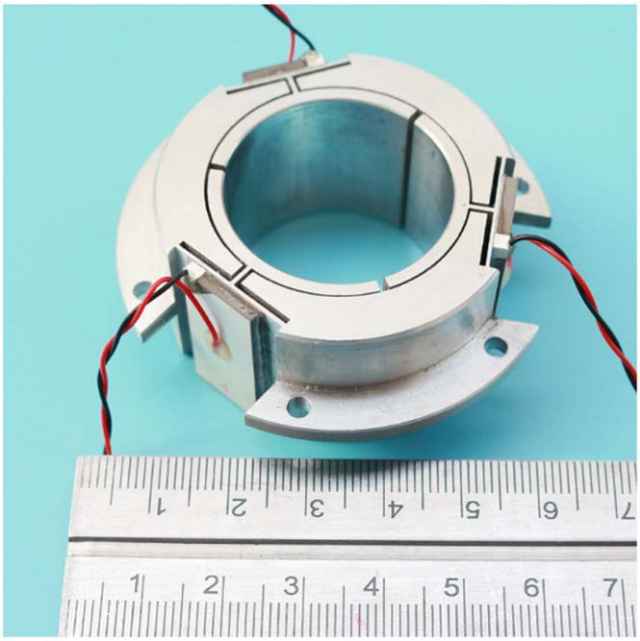

Figure 23. Photograph of squeeze film air bearing: Feng *et al* [132]. Reprinted from [132], Copyright (2017), with permission from Elsevier.

same input voltage. Therefore, resonance frequency and vibration amplitude were also concluded to be two crucial parts for SFAB. However, the vibration amplitude was a more

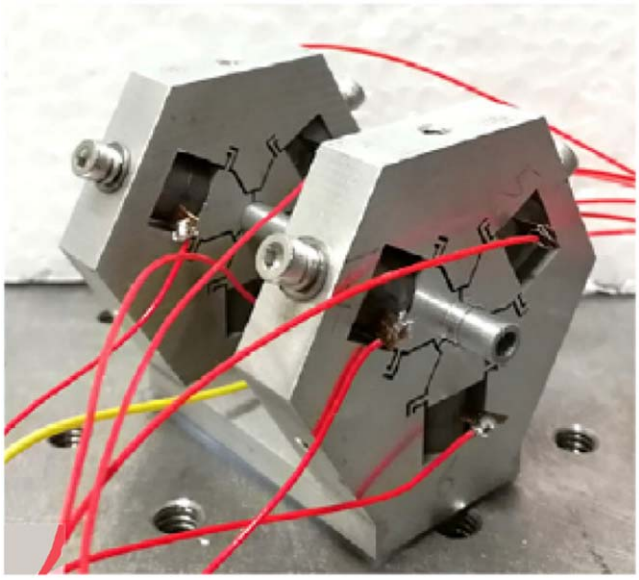

Figure 24. Photograph of non-contact journal bearing: Guo and Cao [135]. Reprinted from [135], Copyright (2018), with permission from Elsevier.

important part than was resonance frequency. The conclusion was a better answer to the question raised by the literature [134].

An active non-contact journal bearing with bidirectional driving capability achieved by using coupled resonant vibration was proposed in [135]. The design of the bearing consisted of three identical horn structures with a concave end surface (reference figure 24). The main feature of this bearing, which was different from the previous ultrasonic bearing, was that it adopted the couple mode shapes, i.e. first longitudinal mode and second bending mode. The alternating work of the longitudinal and bending modes will result in elliptical vibration of the concave end surface. Therefore, vertical levitation and lateral driving force were produced, which supported and rotated the rotor, respectively. It was noticed that the lateral driving force was different from the traveling wave and viscous shear force as it was mainly produced by the tangential component of the squeeze film pressure. Experimental results showed that the rotational speed of $\pm$555 rpm could be obtained by adjusting the input phase angle.

6. Discussion and future trends

The squeeze film effect has been demonstrated to be capable of levitating objects for a wide range of applications. One of the main issues is the influence of governing parameters on the levitation performance and, in particular, the load-carrying capacity. In general, the SFAB system consists of bearing, vibration generators, which are usually piezoelectric transducers, and a signal generating system, which generates signal applied to vibration generators. The performance of SFABs is closely associated with several governing parameters, such as the geometry, materials, resonance frequency, vibration amplitude, and excitation signal value. The geometry plays a crucial role in the SFAB design process because the bearing performance can be remarkably enhanced by choosing an appropriate geometry [121]. In order to obtain ideal bearing performance, the designer should select the appropriate mode shape according to the geometry of the bearing in the design process. Additionally, it is often important to consider the effect of the materials on the load-carrying capacity of the bearing. Studies show that the materials affect the resonance frequency and vibration amplitude of the SFAB, which results in different squeeze film effects [125, 133, 134]. For SFABs, materials with a low energy absorption coefficient and structural stiffness will be a better choice.

With regard to the SFABs, the majority of the research has focused on bearing structure and vibration generator design. The designs of the bearing structure and vibration generator are relatively mature, and the research into bearing structure and vibration generator design for further improvement of the SFAB application in the field of machining is still insufficient since many physical mechanism are not recognized fully. Consequently, the future trends are as follows:

(1) *Greater load-carrying capacity*. In general, the load-carrying capacity of SFABs (only squeeze film effect) is lower that of conventional non-contact bearings. Therefore, the SFAB with greater load-carrying capacity should be developed.
(2) *Coupled modeling of squeeze film systems.* During the operation of SFAB systems, a large amount of heat is generated, which leads to thermal deformations. The squeeze film levitation model with the thermal-fluid-structure interaction effect should be fully investigated theoretically and experimentally, including the influence of heat on fluid and structural deformation.
(3) *Active squeeze film bearings*. Since only a small portion of the literature proposed active squeeze film bearings, there is a need for an in-depth investigation into the running performance of the squeeze film bearing with a closed-loop control system. How to conduct accurate motion control under different working conditions to thoroughly understand the squeeze film levitation system should be further investigated.
(4) *Novel vibration generator*. The vibration generator plays a vital role in squeeze film bearing systems. In order to improve the running performance of the bearing and enhance the efficiency of energy utilization, a novel vibration generator should be developed.
(5) *Different lubricants and expanding industrial application*. Squeeze film bearings with other lubricants are a critical issue that needs to be investigated. Furthermore, the application of squeeze film bearings should not be limited to guideways and machine spindles. Other industrial applications, such as micro turbines, air compressors, and turbochargers, need more attention.

7. Conclusions

Non-contact bearings are core components of ultra-precision machine tools. Research on SFABs, as one of the non-contact bearings, has been ongoing for about decades. This review paper conducted a simple comparison of the four non-contacts bearings by evaluating their run time, stability, friction and wear, motion accuracy, energy consumption, etc. The four kinds of non-contact technologies have their own features and should be selected according to the actual working conditions. This paper introduced the fundamental theory for the performance prediction of SFABs. Different types of squeeze film bearings, including squeeze film linear bearings, thrust bearings, spherical bearings, and journal bearings (hybrid SFABs), are summarized in this paper, and their principles have been briefly introduced.

Although many investigators have studied the SFABs experimentally and numerically, there are still gaps in directly applying SFABs to ultra-precision machine tools. In the future, development of squeeze film bearings with greater load-carrying capacity is expected. Thus, a novel vibration generator should be proposed which could be promoted by potential technologies, including piezoelectric and electromagnetic technologies. In-depth investigation into the squeeze film levitation model with the thermal-fluid-structure interaction effect is also required. In addition, active squeeze film bearings with a closed-loop control system is a further direction for achieving more accurate motion, and other industrial applications should be explored.

Acknowledgments

The authors acknowledge the financial support from the National Natural Science Foundation of China (Nos. 51575170 and 51875185), the National Key R&D Program of China (2018YFB2000100), and the Foundation of Hunan Province (2018JJ1006).

ORCID iDs

Kai Feng https://orcid.org/0000-0002-9287-9379

References

[1] Lee J, Kao H-A and Yang S 2014 Service innovation and smart analytics for industry 4.0 and big data environment *Proc. Cirp.* **16** 3–8
[2] Stock T and Seliger G 2016 Opportunities of sustainable manufacturing in industry 4.0 *Proc. Cirp.* **40** 536–41
[3] Zhong R Y, Xu X, Klotz E and Newman S T 2017 Intelligent manufacturing in the context of industry 4.0: a review *Engineering* **3** 616–30
[4] Kim D-H *et al* 2018 Smart machining process using machine learning: a review and perspective on machining industry *Int. J. Precis. Eng. Manuf.—Green Technol.* **5** 555–68
[5] Gao Q, Chen W, Lu L, Huo D and Cheng K 2019 Aerostatic bearings design and analysis with the application to precision engineering: state-of-the-art and future perspectives *Tribol. Int.* **135** 1–17
[6] Fuller D D 1969 A review of the state-of-the-art for the design of self-acting gas-lubricated bearings *J. Lubr. Technol.* **91** 1–16
[7] Heshmat H and Hermel P 1993 Compliant foil bearings technology and their application to high speed turbomachinery *Tribology Series* (Amsterdam: Elsevier) pp 559–75
[8] DellaCorte C 2008 Technical development path for foil gas bearings *STLE/ASME 2008 Int. Joint Tribology Conf.: American Society of Mechanical Engineers* pp 299–302
[9] Bulat M P and Bulat P V 2013 The history of the gas bearings theory development *World Appl. Sci. J.* **27** 893–7
[10] Bleuler H *et al* 2009 *Magnetic Bearings: Theory, Design, and Application to Rotating Machinery* (Berlin: Springer)
[11] Reynolds O IV 1886 On the theory of lubrication and its application to Mr Beauchamp tower's experiments, including an experimental determination of the viscosity of olive oil *Phil. Trans. R. Soc.* **117** 157–234
[12] Tipei N 1954 Equatiile lubrificatiei cu gaze *Commun. Acad RP Romine* **4** 699
[13] Langlois W 1962 Isothermal squeeze films *Q. Appl. Math.* **20** 131–50
[14] Michael W 1963 Approximate methods for time-dependent gas-film lubrication problems *J. Appl. Mech.* **30** 509–17
[15] Salbu E 1964 Compressible squeeze films and squeeze bearings *J. Basic Eng.* **86** 355–64
[16] Pan C 1967 On asymptotic analysis of gaseous squeeze-film bearings *J. Lubrication Tech.* **89** 245–53
[17] Pan C, Malanoski S, Broussard P and Burch J 1966 Theory and experiments of squeeze-film gas bearings: I. Cylindrical journal bearing *J. Basic Eng.* **88** 191–8
[18] Da Silva F P and Almas E M 1986 Recent developments in the theory of squeeze film bearings *Tribol. Int.* **19** 79–86
[19] Stolarski T A 2014 Acoustic levitation—a novel alternative to traditional lubrication of contacting surfaces *Tribol. Online* **9** 164–74
[20] Andrade M A, Pérez N and Adamowski J C 2018 Review of progress in acoustic levitation *Braz. J. Phys.* **48** 190–213
[21] Vandaele V, Lambert P and Delchambre A 2005 Non-contact handling in microassembly: acoustical levitation *Precis. Eng.* **29** 491–505
[22] Weber R J *et al* 2012 Acoustic levitation: recent developments and emerging opportunities in biomaterials research *Eur. Biophys. J.* **41** 397–403
[23] Priego-Capote F and de Castro L 2006 Ultrasound-assisted levitation: lab-on-a-drop *Trends Anal. Chem.* **25** 856–67
[24] Santesson S and Nilsson S 2004 Airborne chemistry: acoustic levitation in chemical analysis *Anal. Bioanal. Chem.* **378** 1704–9
[25] Gao J, Cao C and Wei B 1999 Containerless processing of materials by acoustic levitation *Adv. Space Res.* **24** 1293–7
[26] Benmore C and Weber J 2011 Amorphization of molecular liquids of pharmaceutical drugs by acoustic levitation *Phys. Rev.* X **1** 011004
[27] Stout K 1985 Design of aerostatic flat pad bearings using annular orifice restrictors *Tribol. Int.* **18** 209–14
[28] Stout K and Rowe W 1972 Analysis of externally-pressurized spherical gas bearings employing slot restrictors *Tribology* **5** 121–7
[29] Nakamura T and Yoshimoto S 1996 Static tilt characteristics of aerostatic rectangular double-pad thrust bearings with compound restrictors *Tribol. Int.* **29** 145–52
[30] Mori H, Yabe H and Ono T 1965 Theory of externally pressurized circular thrust porous gas bearing *J. Basic Eng.* **87** 613–20

[31] Mori H, Miyamatsu Y and Sakata S 1964 Research on externally pressurized circular thrust gas-lubricated bearings *Bull. JSME* **7** 467–73

[32] Kassab S Z, Noureldeen E M and Shawky M A 1997 Effects of operating conditions and supply hole diameter on the performance of a rectangular aerostatic bearing *Tribol. Int.* **30** 533–45

[33] Yoshimoto S, Yamamoto M and Toda K 2007 Numerical calculations of pressure distribution in the bearing clearance of circular aerostatic thrust bearings with a single air supply inlet *J. Tribol.* **129** 384–90

[34] Belforte G, Raparelli T, Viktorov V and Trivella A 2007 Discharge coefficients of orifice-type restrictor for aerostatic bearings *Tribol. Int.* **40** 512–21

[35] Powell J W 1970 *Design of Aerostatic Bearings* (Brighton: Machinery) p 280

[36] Eleshaky M E 2009 CFD investigation of pressure depressions in aerostatic circular thrust bearings *Tribol. Int.* **42** 1108–17

[37] Willis R 1828 On the pressure produced on a flat plate when opposed to a stream of air issuing from an orifice in a plan surface *Trans. Cambridge Phil Soc.* **3** 129–40

[38] Kingsbury A 1897 Experiments with an air-lubricated journal *J. Am. Soc. Naval Eng.* **9** 267–92

[39] Harrison W 1913 The hydrodynamical theory of lubrication with special reference to air as a lubricant *Trans. Camb. Phil. Soc.* **22** 39–54

[40] Katto Y and Soda N 1952 Theory of lubrication by compressible fluid with special reference to air bearing *Proc. 2nd Japan National Congress for Applied Mechanics* pp 267–70

[41] Powell J 1970 A review of progress in gas lubrication *Rev. Phys. Technol.* **1** 96

[42] Ausman J 1963 Linearized ph stability theory for translatory half-speed whirl of long, self-acting gas-lubricated journal bearings *J. Basic Eng.* **85** 611–8

[43] Ausman J 1964 Gas-lubricated bearings *Adv. Bearing Technol.* **38** 109

[44] Castelli V and Pirvics J 1967 Equilibrium characteristics of axial-groove gas-lubricated bearings *J. Lubr. Technol.* **89** 177–93

[45] Cheng H, Castelli V and Chow C 1969 Performance characteristics of spiral-groove and shrouded Rayleigh step profiles for high-speed noncontacting gas seals *J. Lubr. Technol.* **91** 60–8

[46] Bonneau D and Absi J 1994 Analysis of aerodynamic journal bearings with small number of herringbone grooves by finite element method *J. Tribol.* **116** 698–704

[47] Chen X-D and He X-M 2006 The effect of the recess shape on performance analysis of the gas-lubricated bearing in optical lithography *Tribol. Int.* **39** 1336–41

[48] Liu F, Lu Y, Zhang Q, Zhang Y, Gupta P and Müller N 2016 Load performance analysis of three-pad fixing pad aerodynamic journal bearings with parabolic grooves *Lubr. Sci.* **28** 207–20

[49] Gunter E Jr, Hinkle J and Fuller D 1964 The effects fo speed, load, and film thickness on the performance of gas-lubricated, tilting-pad journal bearings *ASLE Trans.* **7** 353–65

[50] San Andrés L 2006 Hybrid flexure pivot-tilting pad gas bearings: analysis and experimental validation *J. Tribol.* **128** 551–8

[51] Sim K and Kim D 2007 Design of flexure pivot tilting pads gas bearings for high-speed oil-free microturbomachinery *J. Tribol.* **129** 112–9

[52] Lihua Y, Shemiao Q and Lie Y 2009 Analysis on dynamic performance of hydrodynamic tilting-pad gas bearings using partial derivative method *J. Tribol.* **131** 011703

[53] Heshmat C and Heshmat H 1995 An analysis of gas-lubricated, multileaf foil journal bearings with backing springs *J. Tribol.* **117** 437–43

[54] Kim D 2007 Parametric studies on static and dynamic performance of air foil bearings with different top foil geometries and bump stiffness distributions *J. Tribol.* **129** 354–64

[55] DellaCorte C, Radil K C, Bruckner R J and Howard S A 2008 Design, fabrication, and performance of open source generation I and II compliant hydrodynamic gas foil bearings *Tribol. Trans.* **51** 254–64

[56] Kim T H and Andres L S 2009 Effects of a mechanical preload on the dynamic force response of gas foil bearings: measurements and model predictions *Tribol. Trans.* **52** 569–80

[57] Feng K and Kaneko S 2010 Analytical model of bump-type foil bearings using a link-spring structure and a finite-element shell model *J. Tribol.* **132** 021706

[58] Kaplan B 1970 Recent developments in magnetic levitation *Electron. Lett.* **6** 230–1

[59] Atherton D 1980 Maglev using permanent magnets *IEEE Trans. Magn.* **16** 146–8

[60] Azukizawa T, Yamamoto S and Matsuo N 2008 Feasibility study of a passive magnetic bearing using the ring shaped permanent magnets *IEEE Trans. Magn.* **44** 4277–80

[61] Moser R, Sandtner J and Bleuler H 2006 Optimization of repulsive passive magnetic bearings *IEEE Trans. Magn.* **42** 2038–42

[62] Yonnet J-P 1978 Passive magnetic bearings with permanent magnets *IEEE Trans. Magn.* **14** 803–5

[63] Schweitzer G 2002 Active magnetic bearings-chances and limitations *IFToMM 6th Int. Conf. on Rotor Dynamics (Sydney, Australia)* (Citeseer) pp 1–14

[64] Lei S and Palazzolo A 2008 Control of flexible rotor systems with active magnetic bearings *J. Sound Vib.* **314** 19–38

[65] Khoo W, Kalita K, Garvey S D, Hill-Cottingham R, Rodger D and Eastham J F 2010 Active axial-magnetomotive force parallel-airgap serial flux magnetic bearings *IEEE Trans. Magn.* **46** 2596–602

[66] Kim H-Y and Lee C-W 2004 Analysis of eddy-current loss for design of small active magnetic bearings with solid core and rotor *IEEE Trans. Magn.* **40** 3293–301

[67] Yanliang X, Yueqin D, Xiuhe W and Yu K 2006 Analysis of hybrid magnetic bearing with a permanent magnet in the rotor by FEM *IEEE Trans. Magn.* **42** 1363–6

[68] Jiancheng F, Jinji S, Yanliang X and Xi W 2009 A new structure for permanent-magnet-biased axial hybrid magnetic bearings *IEEE Trans. Magn.* **45** 5319–25

[69] Jiancheng F, Jinji S, Hu L and Jiqiang T 2010 A novel 3-DOF axial hybrid magnetic bearing *IEEE Trans. Magn.* **46** 4034–45

[70] Beck J V and Strodtman C 1968 Load support of the squeeze-film journal bearing of finite length *J. Lubr. Technol.* **90** 157–61

[71] DiPrima R C 1968 Asymptotic methods for an infinitely long slider squeeze-film bearing *J. Lubr. Technol.* **90** 173–83

[72] Takada H, Kamigaichi S and Miura H 1983 Characteristics of squeeze air film between nonparallel plates *J. Lubr. Technol.* **105** 147–52

[73] Beck J V, Holliday W and Strodtman C 1969 Experiment and analysis of a flat disk squeeze-film bearing including effects of supported mass motion *J. Lubr. Technol.* **91** 138–48

[74] Yoshimoto S, Anno Y, Sato Y and Hamanaka K 1997 Float characteristics of squeeze-film gas bearing with elastic hinges for linear motion guide *JSME Int. J.* C **40** 353–9

[75] Stolarski T and Chai W 2006 Load-carrying capacity generation in squeeze film action *Int. J. Mech. Sci.* **48** 736–41

[76] Mahajan M, Jackson R and Flowers G 2008 Experimental and analytical investigation of a dynamic gas squeeze film bearing including asperity contact effects *Tribol. Trans.* **51** 57–67

[77] Ha D, Stolarski T and Yoshimoto S 2005 An aerodynamic bearing with adjustable geometry and self-lifting capacity: I. Self-lift capacity by squeeze film *Proc. Inst. Mech. Eng.* J **219** 33–9

[78] Yoshimoto S, Kobayashi H and Miyatake M 2007 Float characteristics of a squeeze-film air bearing for a linear motion guide using ultrasonic vibration *Tribol. Int.* **40** 503–11

[79] Liu P, Li J, Ding H and Cao W 2009 Modeling and experimental study on near-field acoustic levitation by flexural mode *IEEE Trans. Ultrason. Ferroelectr. Freq. Control* **56** 2679–85

[80] Wang Y and Wei B 2013 Mixed-modal disk gas squeeze film theoretical and experimental analysis *Int. J. Mod. Phys.* B **27** 1350168

[81] Ilssar D, Bucher I and Flashner H 2017 Modeling and closed loop control of near-field acoustically levitated objects *Mech. Syst. Signal Process.* **85** 367–81

[82] Kang J, Xu Z and Akay A 1995 Inertia effects on compressible squeeze films *Trans. ASME. J. Vib. Acoust.* **117** 94

[83] Hashimoto H 1995 Squeeze film characteristics between parallel circular plates containing a single central air bubble in the inertial flow regime *J. Tribol.* **117** 513–8

[84] Stolarski T and Chai W 2008 Inertia effect in squeeze film air contact *Tribol. Int.* **41** 716–23

[85] Li J, Cao W, Liu P and Ding H 2010 Influence of gas inertia and edge effect on squeeze film in near field acoustic levitation *Appl. Phys. Lett.* **96** 243507

[86] Nomura H, Kamakura T and Matsuda K 2002 Theoretical and experimental examination of near-field acoustic levitation *J. Acoust. Soc. Am.* **111** 1578–83

[87] Minikes A, Bucher I and Haber S 2004 Levitation force induced by pressure radiation in gas squeeze films *J. Acoust. Soc. Am.* **116** 217–26

[88] Minikes A and Bucher I 2003 Coupled dynamics of a squeeze-film levitated mass and a vibrating piezoelectric disc: numerical analysis and experimental study *J. Sound Vib.* **263** 241–68

[89] Minikes A and Bucher I 2006 Comparing numerical and analytical solutions for squeeze-film levitation force *J. Fluids Struct.* **22** 713–9

[90] Li W, Liu Y and Feng K 2017 Modelling and experimental study on the influence of surface grooves on near-field acoustic levitation *Tribol. Int.* **116** 138–46

[91] Gross W A 1962 *Gas Film Lubrication* (New York: Wiley)

[92] Rayleigh L 1902 XXXIV. On the pressure of vibrations *London, Edinburgh, Dublin Phil. Mag. J. Sci.* **3** 338–46

[93] Post E 1953 Radiation pressure and dispersion *J. Acoust. Soc. Am.* **25** 55–60

[94] Rooney J A and Nyborg W L 1972 Acoustic radiation pressure in a traveling plane wave *Am. J. Phys.* **40** 1825–30

[95] Beyer R T 1978 Radiation pressure—the history of a mislabeled tensor *J. Acoust. Soc. Am.* **63** 1025–30

[96] Livett A, Emery E and Leeman S 1981 Acoustic radiation pressure *J. Sound Vib.* **76** 1–11

[97] Chu B T and Apfel R E 1982 Acoustic radiation pressure produced by a beam of sound *J. Acoust. Soc. Am.* **72** 1673–87

[98] Lee C and Wang T 1993 Acoustic radiation pressure *J. Acoust. Soc. Am.* **94** 1099–109

[99] Hashimoto Y, Koike Y and Ueha S 1996 Near-field acoustic levitation of planar specimens using flexural vibration *J. Acoust. Soc. Am.* **100** 2057–61

[100] Ueha S, Hashimoto Y and Koike Y 2000 Non-contact transportation using near-field acoustic levitation *Ultrasonics* **38** 26–32

[101] Zhao S, Mojrzisch S and Wallaschek J 2013 An ultrasonic levitation journal bearing able to control spindle center position *Mech. Syst. Signal Process.* **36** 168–81

[102] Melikhov I, Chivilikhin S, Amosov A and Jeanson R 2016 Viscoacoustic model for near-field ultrasonic levitation *Phys. Rev.* E **94** 053103

[103] Yoshimoto S 1993 Rectangular squeeze-film gas bearing using a piezoelectric actuator-application to a linear motion guide *Int. J. JSPE* **27** 259

[104] Yoshimoto S 1997 Floating characteristics of squeeze-film gas bearings with vibration absorber for linear motion guide. transactions-American society of mechanical engineers *J. Tribol.* **119** 531–6

[105] Stolarski T and Chai W 2006 Self-levitating sliding air contact *Int. J. Mech. Sci.* **48** 601–20

[106] Wiesendanger M 2001 *Squeeze Film Air Bearings using Piezoelectric Bending Elements* (Verlag Nicht Ermittelbar)

[107] Ide T, Friend J R, Nakamura K and Ueha S 2005 A low-profile design for the noncontact ultrasonically levitated stage *Japan. J. Appl. Phys.* **44** 4662

[108] Ide T, Friend J, Nakamura K and Ueha S 2007 A non-contact linear bearing and actuator via ultrasonic levitation *Sensors Actuators* A **135** 740–7

[109] Koyama D, Ide T, Friend J R, Nakamura K and Ueha S 2005 An ultrasonically levitated non-contact sliding table with the traveling vibrations on fine-ceramic beams *IEEE Ultrasonics Symp., 2005* (IEEE) pp 1538–41

[110] Oiwa T and Suzuki R 2005 Linear rectangular air bearing based on squeeze film generated by ultrasonic oscillation *Rev. Sci. Instrum.* **76** 075101

[111] Shiju E, Jiang X, Cao J, Ge C, Liu A and Jin L 2015 Experimental research on levitation mechanism of ultrasonic bearing *2015 IEEE Int. Conf. on Information and Automation* (IEEE) pp 100–5

[112] Song Y G *et al* 2013 Experimental research on the levitation support way of ultrasonic thrust bearing *Appl. Mech. Mater.: Trans. Tech. Publ.* **423** 1571–6

[113] Liu J-F, Sun X-G, Jiao X-Y, Chen H-X, Hua S-M and Zhang H-C 2013 The near-field acoustic levitation for spheres by transducer with concave spherical radiating surface *J. Mech. Sci. Technol.* **27** 289–95

[114] Hong Z, Lü P, Geng D, Zhai W, Yan N and Wei B 2014 The near-field acoustic levitation of high-mass rotors *Rev. Sci. Instrum.* **85** 104904

[115] Lü P, Hong Z, Yin J, Yan N, Zhai W and Wang H 2016 Note: attenuation motion of acoustically levitated spherical rotor *Rev. Sci. Instrum.* **87** 116103

[116] Chen C, Wang J, Jia B and Li F 2014 Design of a noncontact spherical bearing based on near-field acoustic levitation *J. Intell. Mater. Syst. Struct.* **25** 755–67

[117] Farron J R and Teitelbaum B R 1969 Squeeze film bearings *US Patent* 3,471,205

[118] Emmerich C L 1967 Piezoelectric oscillating bearing *US Patent* 3,351,393

[119] Hu J, Nakamura K and Ueha S 1997 An analysis of a noncontact ultrasonic motor with an ultrasonically levitated rotor *Ultrasonics* **35** 459–67

[120] Oiwa T and Kato M 2004 Squeeze air bearing based on ultrasonic oscillation: motion error compensation using amplitude modulation *Rev. Sci. Instrum.* **75** 4615–20

[121] Stolarski T, Gawarkiewicz R and Tesch K 2015 Acoustic journal bearing—a search for adequate configuration *Tribol. Int.* **92** 387–94

[122] Stolarski T A 2011 Running characteristics of aerodynamic bearing with self-lifting capability at low rotational speed *Adv. Tribol.* **2011** 973740

[123] Feng K, Shi M, Gong T and Huang Z 2018 Integrated numerical analysis on the performance of a hybrid gas-lubricated bearing utilizing near-field acoustic levitation *Tribol. Trans.* **61** 482–93
[124] Stolarski T, Gawarkiewicz R and Tesch K 2017 Extended duration running and impulse loading characteristics of an acoustic bearing with enhanced geometry *Tribol. Lett.* **65** 46
[125] Stolarski T, Xue Y and Yoshimoto S 2011 Air journal bearing utilizing near-field acoustic levitation stationary shaft case *Proc. Inst. Mech. Eng.* J **225** 120–7
[126] Shou T, Yoshimoto S and Stolarski T 2013 Running performance of an aerodynamic journal bearing with squeeze film effect *Int. J. Mech. Sci.* **77** 184–93
[127] Wang C and Au Y 2011 Study of design parameters for squeeze film air journal bearing–excitation frequency and amplitude *Mech. Sci.* **2** 147–55
[128] Wang J-S, Chen C, Chen G-C and Yan X-J 2013 Research on a new type of ultrasonic bearing based on near field acoustic levitation *2013 Symp. on Piezoelectricity, Acoustic Waves, and Device Applications* (IEEE) pp 1–4
[129] Li H, Quan Q, Deng Z, Hua Y, Wang Y and Bai D 2016 A novel noncontact ultrasonic levitating bearing excited by piezoelectric ceramics *Appl. Sci.* **6** 280
[130] Li H, Quan Q, Deng Z, Bai D and Wang Y 2018 Design and experimental study on an ultrasonic bearing with bidirectional carrying capacity *Sensors Actuators* A **273** 58–66
[131] Li H and Deng Z 2018 Experimental study on friction characteristics and running stability of a novel ultrasonic levitating bearing *IEEE Access.* **6** 21719–30
[132] Feng K, Shi M, Gong T, Liu Y and Zhu J 2017 A novel squeeze-film air bearing with flexure pivot-tilting pads: numerical analysis and measurement *Int. J. Mech. Sci.* **134** 41–50
[133] Shi M, An L, Feng K, Guo Z and Liu W 2018 Numerical and experimental study on the influence of material characteristics on the levitation performance of squeeze-film air bearing *Tribol. Int.* **126** 307–16
[134] Wang C and Au Y J 2013 Comparative performance of squeeze film air journal bearings made of aluminium and copper *Int. J. Adv. Manuf. Technol.* **65** 57–66
[135] Guo P and Gao H 2018 An active non-contact journal bearing with bi-directional driving capability utilizing coupled resonant mode *CIRP Ann.* **67** 405–8